Effect of rotation zero-crossing on plasma response to 3D magnetic perturbations

Brendan Carrick Lyons[1,2]

N.M. Ferraro[3], C. Paz-Soldan[2], R. Nazikian[3], A. Wingen[4]

[1] Oak Ridge Institute for Science and Education
[2] General Atomics
[3] Princeton Plasma Physics Laboratory
[4] Oak Ridge National Laboratory

Center for Extended MHD Modeling Meeting
San Jose, California
October 30th, 2016

OAK RIDGE INSTITUTE FOR SCIENCE AND EDUCATION
Managed by ORAU for DOE

GENERAL ATOMICS

Theory of ELM suppression by 3D fields still incomplete

- **External 3D magnetic perturbations are routinely used to mitigate or to suppress edge-localized modes (ELMs)**
- **Early theoretical work predicted that**
  - Vacuum fields would produce overlapping islands in edge
  - Stochastic transport would inhibit pedestal growth
- **Recent results inconsistent with formation of stochastic layer**
  - Electron temperature gradient not observed to decrease
  - Electron rotation predicted to screen vacuum islands in edge
- **Current theory requires on island opening only at pedestal top**
  - Observed that zero-crossing of electron rotation aligns with rational surface at top of pedestal during suppression
  - Theory predicts
    - Low rotation permits penetration of resonant field
    - Island arrests growth of pedestal height and width

Extended-MHD analysis can inform this theory

- **Comprehensive model needed for pedestal evolution across ELM-suppression bifurcation**
  - Extended MHD
    - Time-dependent (for evolution)
    - Nonlinear (for island saturation)
    - Two-fluid (for electron rotation physics)
  - Appropriate transport model, particularly for the momentum
- **Current research focuses on individual components of model**
- **Here, we explore how rotation profiles affect single-fluid M3D-C1 plasma response, including**
  - Resonant field
  - Non-resonant field
  - Observable quantities
  - Quasilinear electromagnetic torque

M3D-C1 [1] solves the extended MHD equations

- **Three-dimensional**
- **Includes resistivity, density diffusivity, viscosity, & thermal conductivity**
- **Two-fluid effects (optional)**
- **Linear and nonlinear modes**
- **High-order, C^1 continuous finite element representation**
- **Mesh adapted to input equilibrium**

$$\frac{\partial n_i}{\partial t} + \nabla \cdot (n_i \vec{v}) = 0$$

$$m_i n_i \left[\frac{\partial \vec{v}}{\partial t} + \vec{v} \cdot \nabla \vec{v}\right] = \vec{J} \times \vec{B} - \nabla p - \nabla \cdot \Pi_i$$

$$\frac{\partial \vec{B}^p}{\partial t} = -\nabla \times \vec{E}$$

$$\vec{E} = \eta \vec{J} - \vec{v} \times \vec{B} + \frac{1}{n_e e}(\vec{J} \times \vec{B} - \nabla p_e)$$

$$\Pi = -\mu(\nabla \vec{v} + \nabla \vec{v}^t) + \Pi_i^{\parallel} + \Pi_i^{\wedge}$$

$$\frac{\partial p}{\partial t} + \vec{v} \cdot \nabla p + \Gamma p \nabla \cdot \vec{v} = (\Gamma - 1)\left(\eta J^2 - \nabla \cdot \vec{q} - \Pi_i : \vec{v}\right) + \frac{1}{n_e e}\vec{J} \cdot \left(\nabla p_e - \Gamma \frac{\nabla n_i}{n_i} p_e\right)$$

$$\frac{\partial p_e}{\partial t} + \vec{v} \cdot \nabla p_e + \Gamma p_e \nabla \cdot \vec{v} = (\Gamma - 1)\left(\eta J^2 - \nabla \cdot \vec{q}_e\right) + \frac{1}{n_e e}\vec{J} \cdot \left(\nabla p_e - \Gamma \frac{\nabla n_i}{n_i} p_e\right)$$

$$\vec{q}_{e,i} = -\kappa \nabla T_e - \kappa_{\parallel} \frac{\vec{B}\vec{B}}{B^2} \cdot \nabla T_e \qquad \vec{q} = -\kappa \nabla (T_e + T_i)$$

[2]

[1] S. C. Jardin, et al., Comput. Sci. Discovery 5, 014002 (2012).
[2] N.M. Ferraro et al., Phys. Plasmas 23, 056114 (2016)

M3D-C1 allows for extended MHD simulations of the plasma response to applied 3D fields

- **Plasma response calculations presented here**
  - Linear n=2 (single toroidal mode number)
  - Single-fluid
  - Mesh adapted to equilibrium
  - Resistive wall model allows for free-boundary-like simulations
- **Time-independent 3D equilibrium calculated in response to static perturbation field**

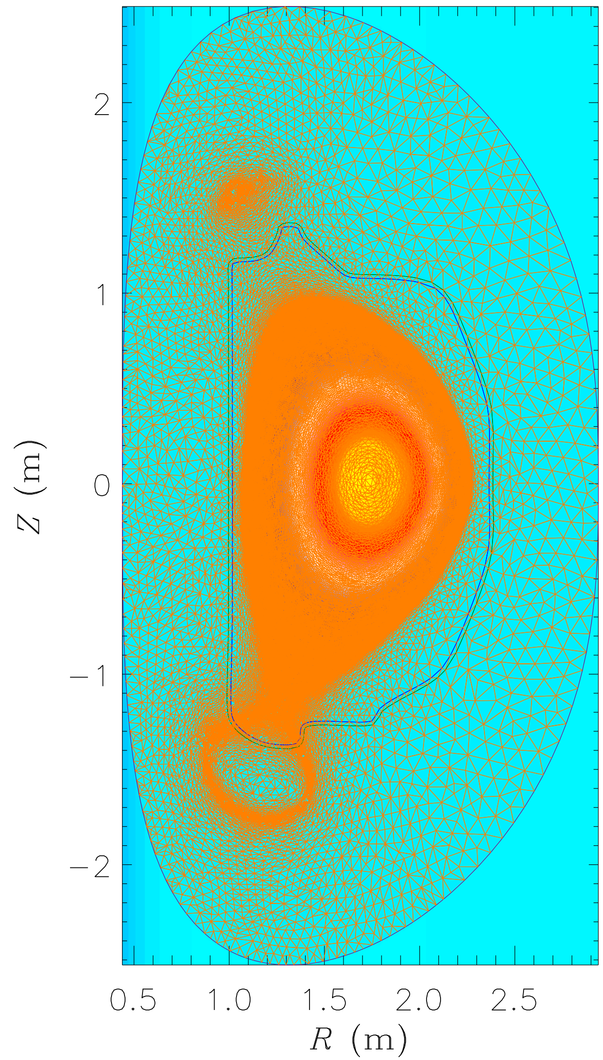

M3D-C1 allows for extended MHD simulations of the plasma response to applied 3D fields

- **Plasma response calculations presented here**
  - Linear n=2 (single toroidal mode number)
  - Single-fluid
  - Mesh adapted to equilibrium
  - Resistive wall model allows for free-boundary-like simulations
- **Time-independent 3D equilibrium calculated in response to static perturbation field**

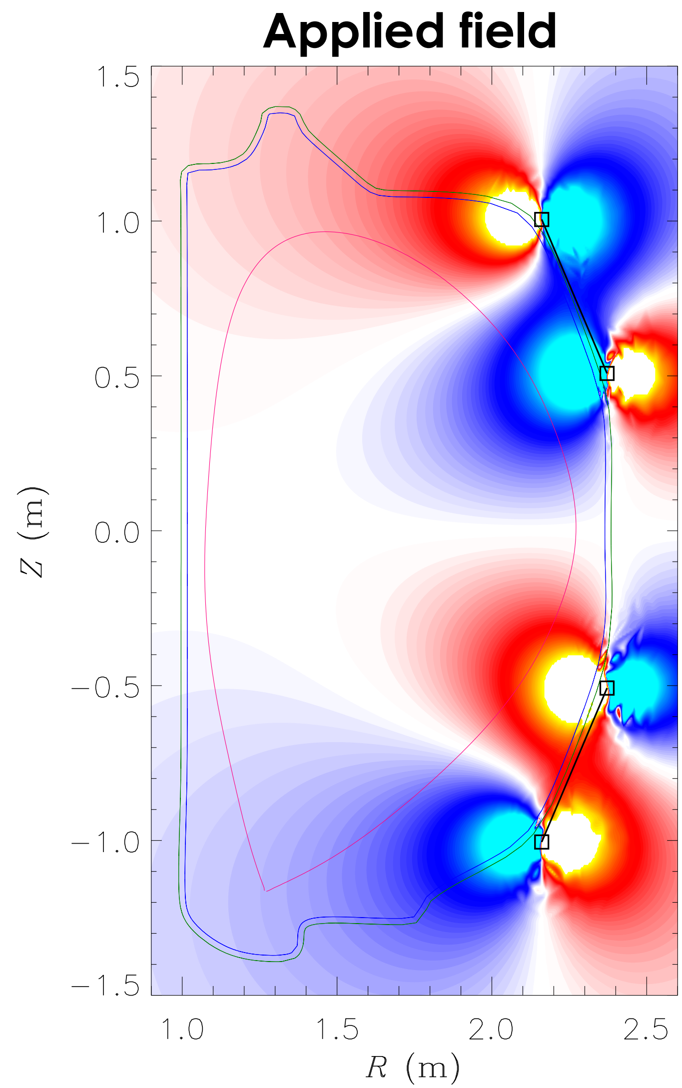

M3D-C1 allows for extended MHD simulations of the plasma response to applied 3D fields

- **Plasma response calculations presented here**
  - Linear n=2 (single toroidal mode number)
  - Single-fluid
  - Mesh adapted to equilibrium
  - Resistive wall model allows for free-boundary-like simulations
- **Time-independent 3D equilibrium calculated in response to static perturbation field**

Plasma response

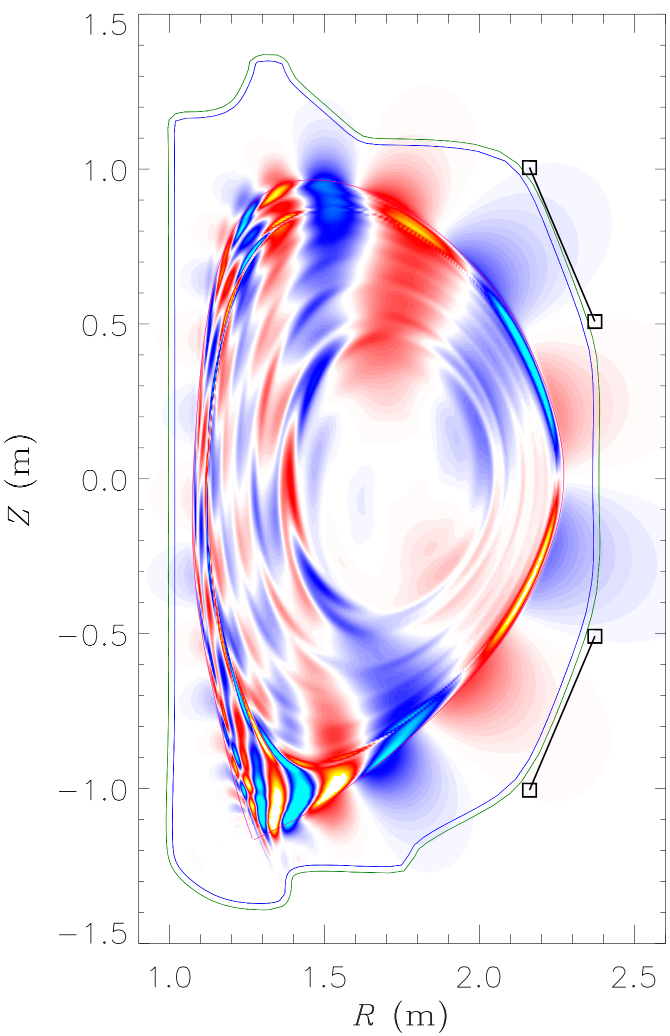

Fourier spectrum provides insight to plasma response

- **Fourier field decomposition:** $\delta B_{mn}(\Psi) = \frac{(2\pi)^2}{A} \iint \frac{\delta \mathbf{B} \cdot \nabla \psi}{\mathbf{B} \cdot \nabla \theta} e^{i(m\theta - n\varphi)} d\theta d\varphi$
- **These SURFMN-like diagrams show magnitude of Fourier components**
  - m - Discrete poloidal harmonic on x-axis
  - Ψ - Continuous normalized poloidal flux on y-axis (radial variable)
  - Resonant m=nq line

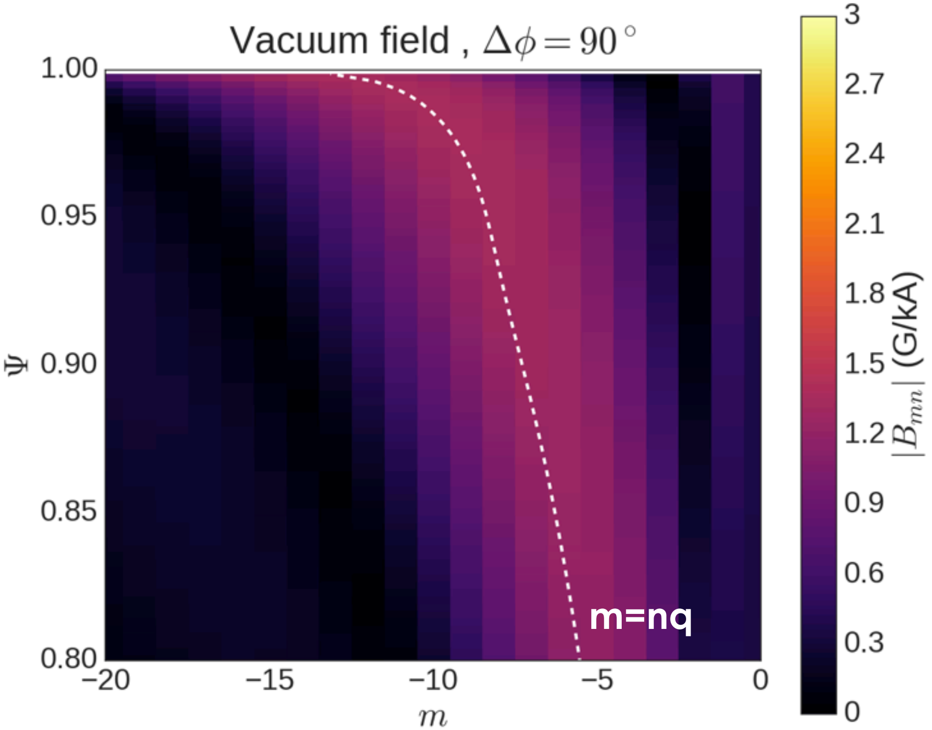

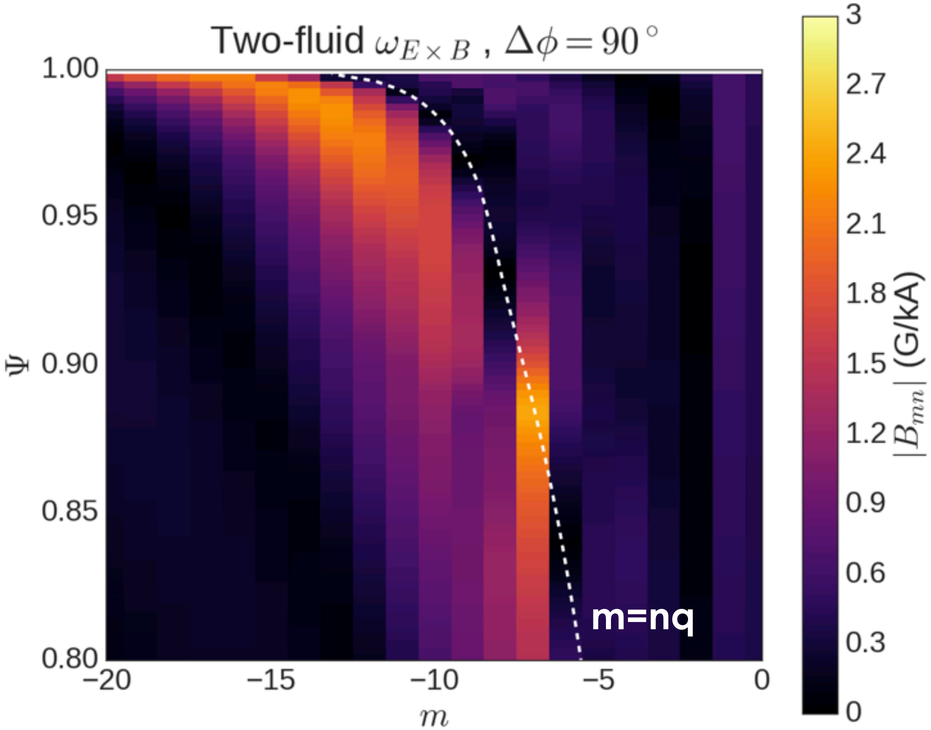

OAK RIDGE INSTITUTE FOR SCIENCE AND EDUCATION
Managed by ORAU for DOE

GENERAL ATOMICS

Plasma response alters perturbed magnetic spectrum

- **Resonant response at rational surfaces (m=nq)**
  - Screening suppresses
  - Tearing enhances
- **Kink response amplifies non-resonant fields with m>nq**

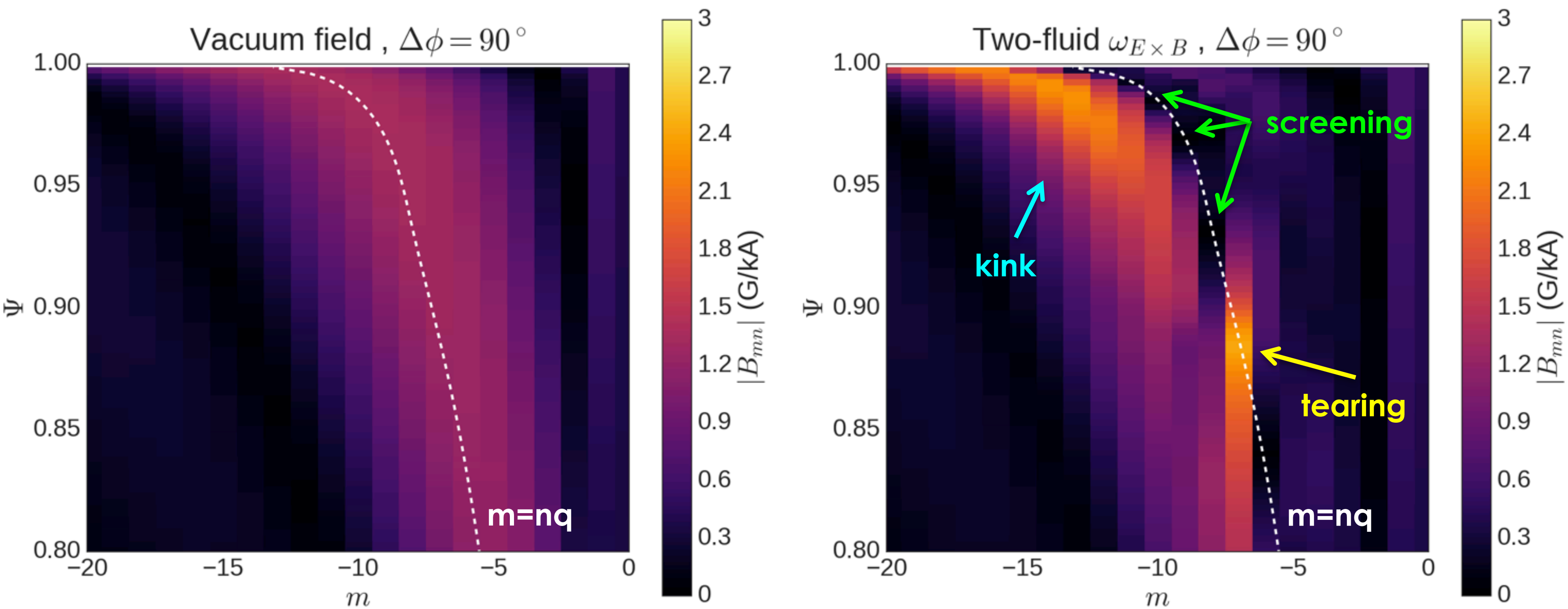

Rotation scan

Past experiments & simulations motivate rotation scan

- **Rotation profile changes during ELM suppression**
  - Zero-crossing of ExB and/or electron rotation often aligns with rational surface during ELM suppression
  - Generally leads to increased tearing drive
- **Single-fluid rotation profile affects verification & validation with external magnetics**
  - M3D-C1 w/ ExB rotation agrees better with data
  - M3D-C1 w/ carbon toroidal rotation agrees better with MARS-F results with same rotation

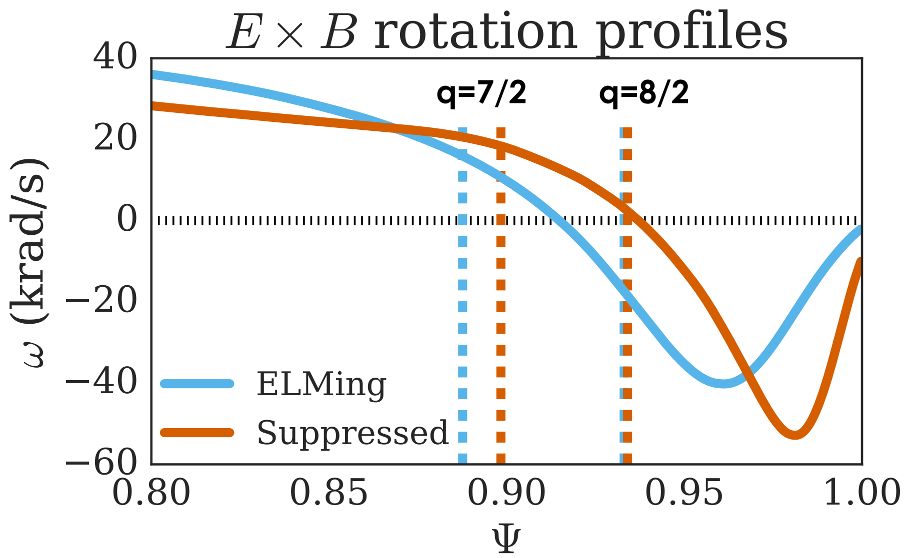

OAK RIDGE INSTITUTE FOR SCIENCE AND EDUCATION
Managed by ORAU for DOE

GENERAL ATOMICS

Past experiments & simulations motivate rotation scan

- **Rotation profile changes during ELM suppression**
  - Zero-crossing of ExB and/or electron rotation often aligns with rational surface during ELM suppression
  - Generally leads to increased tearing drive
- **Single-fluid rotation profile affects verification & validation with external magnetics**
  - M3D-C1 w/ ExB rotation agrees better with data
  - M3D-C1 w/ carbon toroidal rotation agrees better with MARS-F results with same rotation

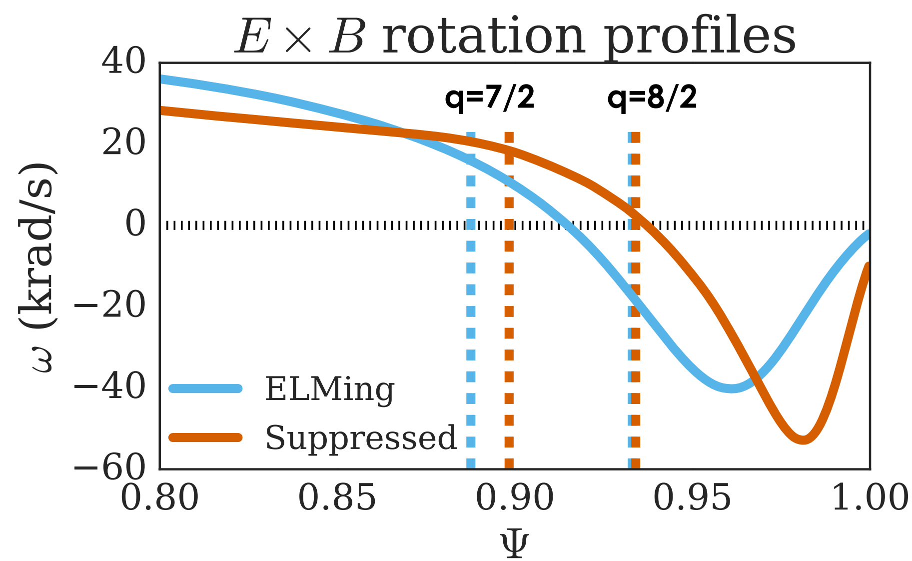

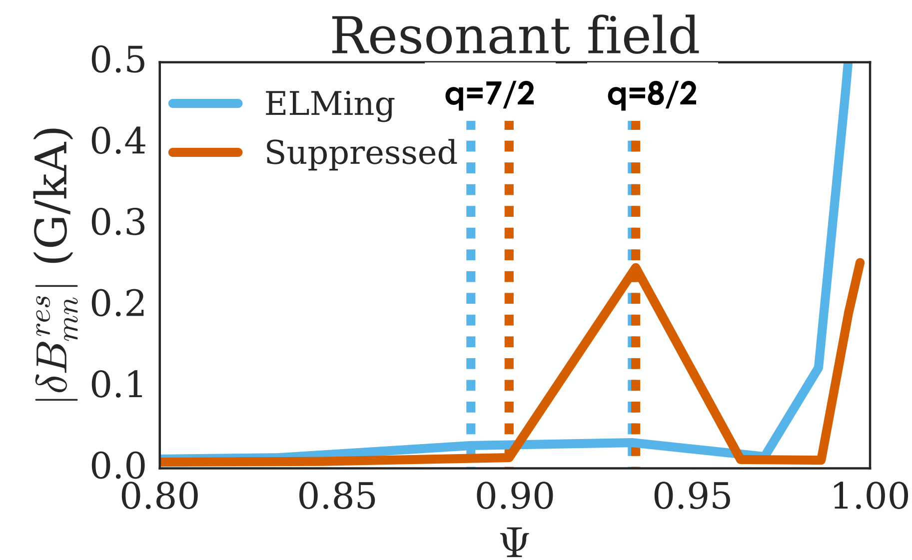

OAK RIDGE INSTITUTE FOR SCIENCE AND EDUCATION
Managed by ORAU for DOE

GENERAL ATOMICS

Past experiments & simulations motivate rotation scan

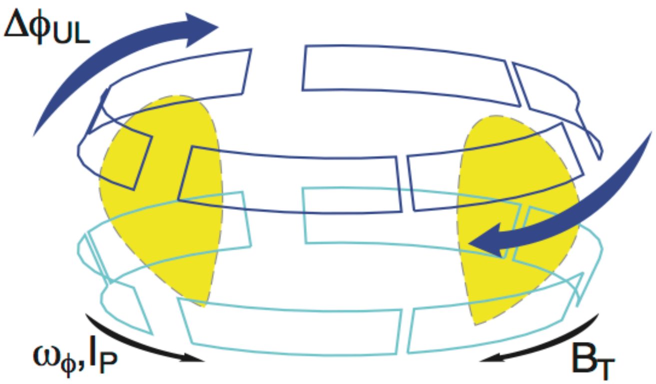

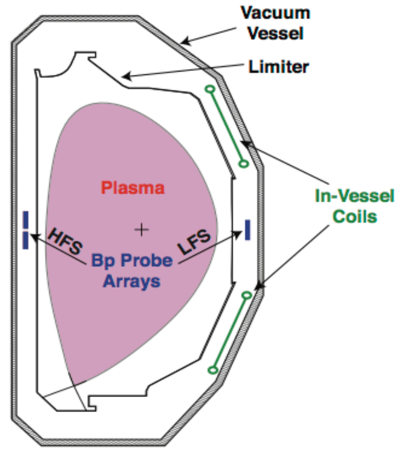

- **Single-fluid rotation profile affects verification & validation with external magnetics**
  - M3D-C1 w/ ExB rotation agrees better with data
  - M3D-C1 w/ carbon toroidal rotation agrees better with MARS-F results with same rotation

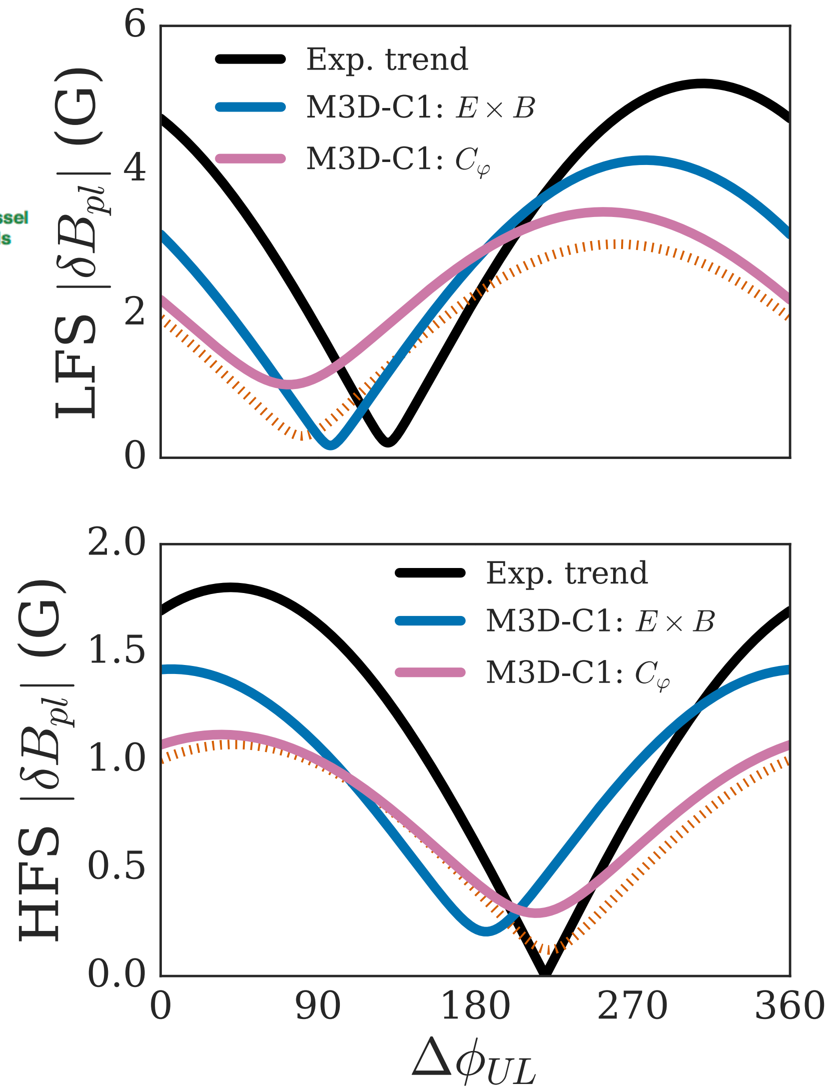

Past experiments & simulations motivate rotation scan

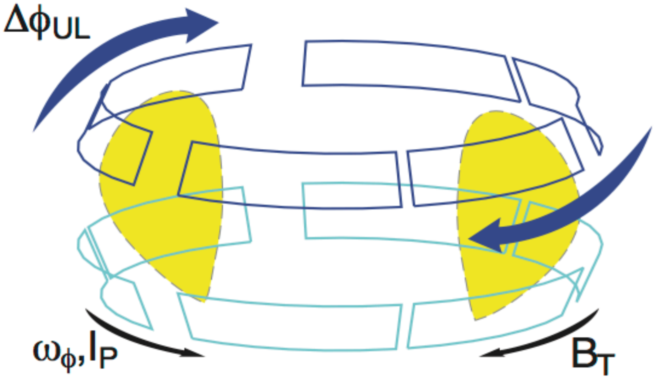

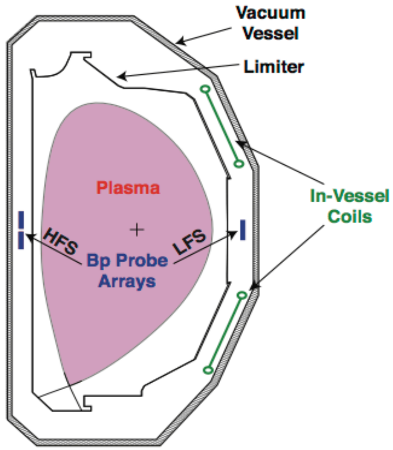

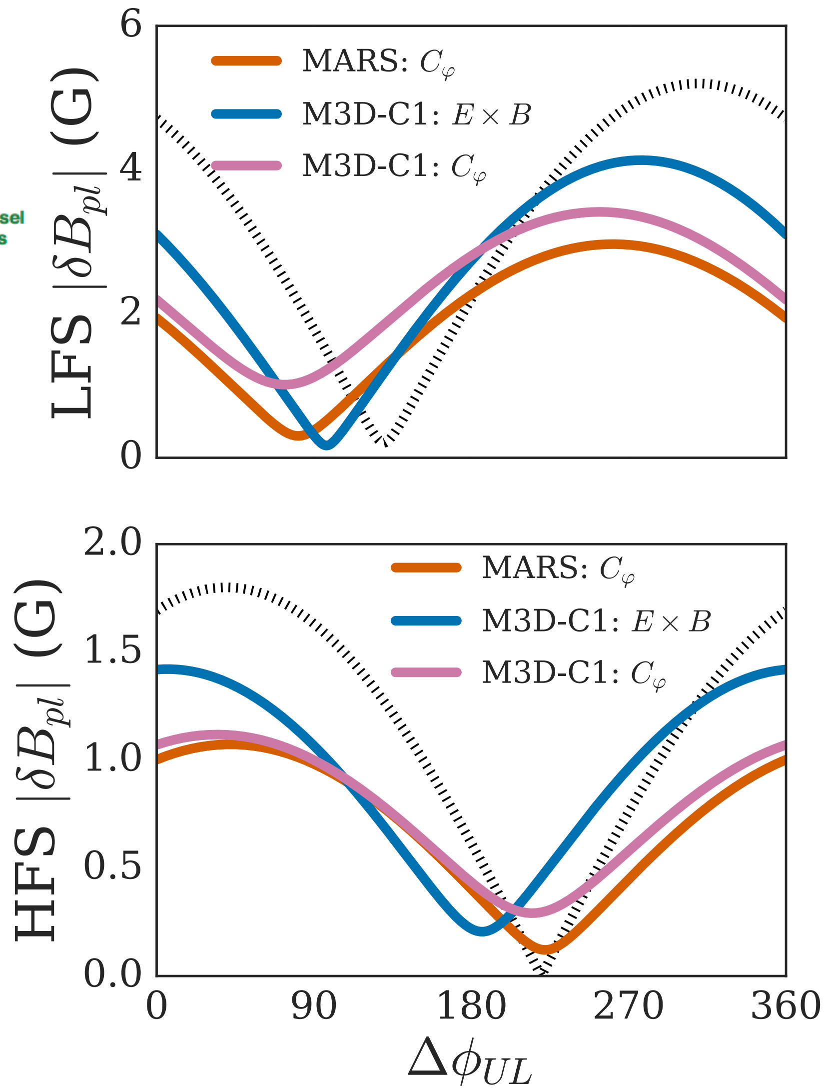

- **Single-fluid rotation profile affects verification & validation with external magnetics**
  - M3D-C1 w/ ExB rotation agrees better with data
  - M3D-C1 w/ carbon toroidal rotation agrees better with MARS-F results with same rotation

Effect of rotation zero-crossing can be tested with systematic variation of model rotation profile

- **DIII-D ITER-similar shape (ISS) equilibrium**
  - Experimental shape and kinetic profiles
- **Model rotation profile with convenient parameterization, including**
  - Zero-crossing: Ψ_z
  - Width of tanh: $\Delta\Psi$ (controls shear)
- **Linear M3D-C1 used to assess effect of rotation on plasma response**

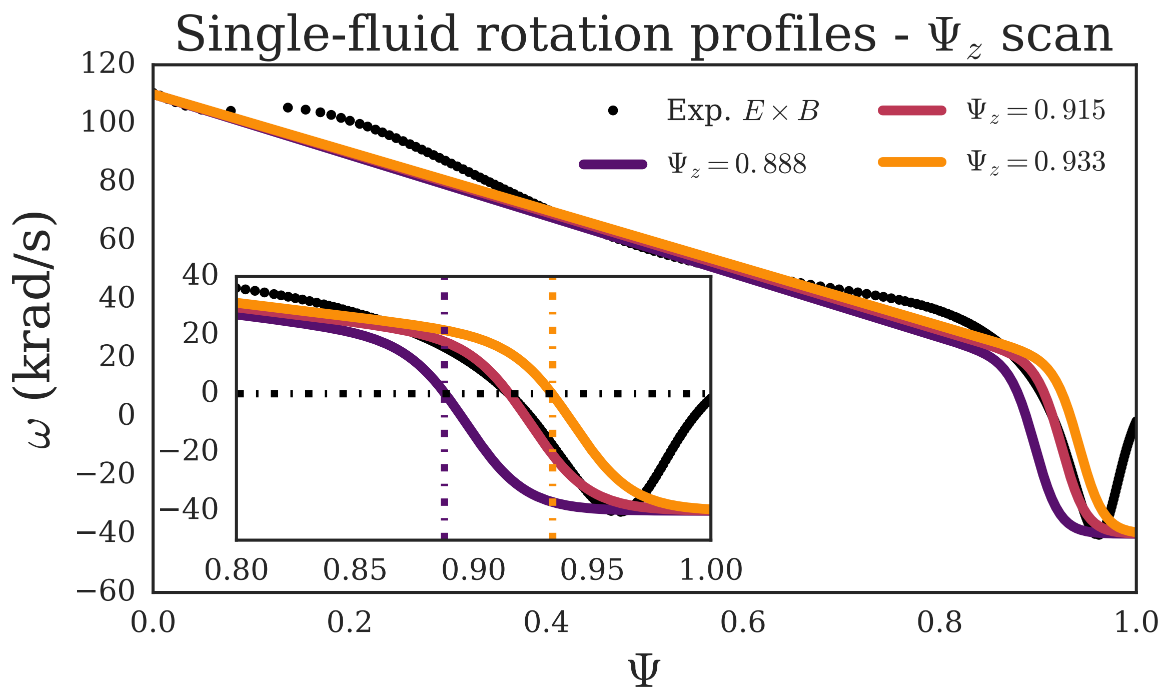

OAK RIDGE INSTITUTE FOR SCIENCE AND EDUCATION
Managed by ORAU for DOE

GENERAL ATOMICS

Effect of zero-crossing on plasma response

Low rotation increases resonant response

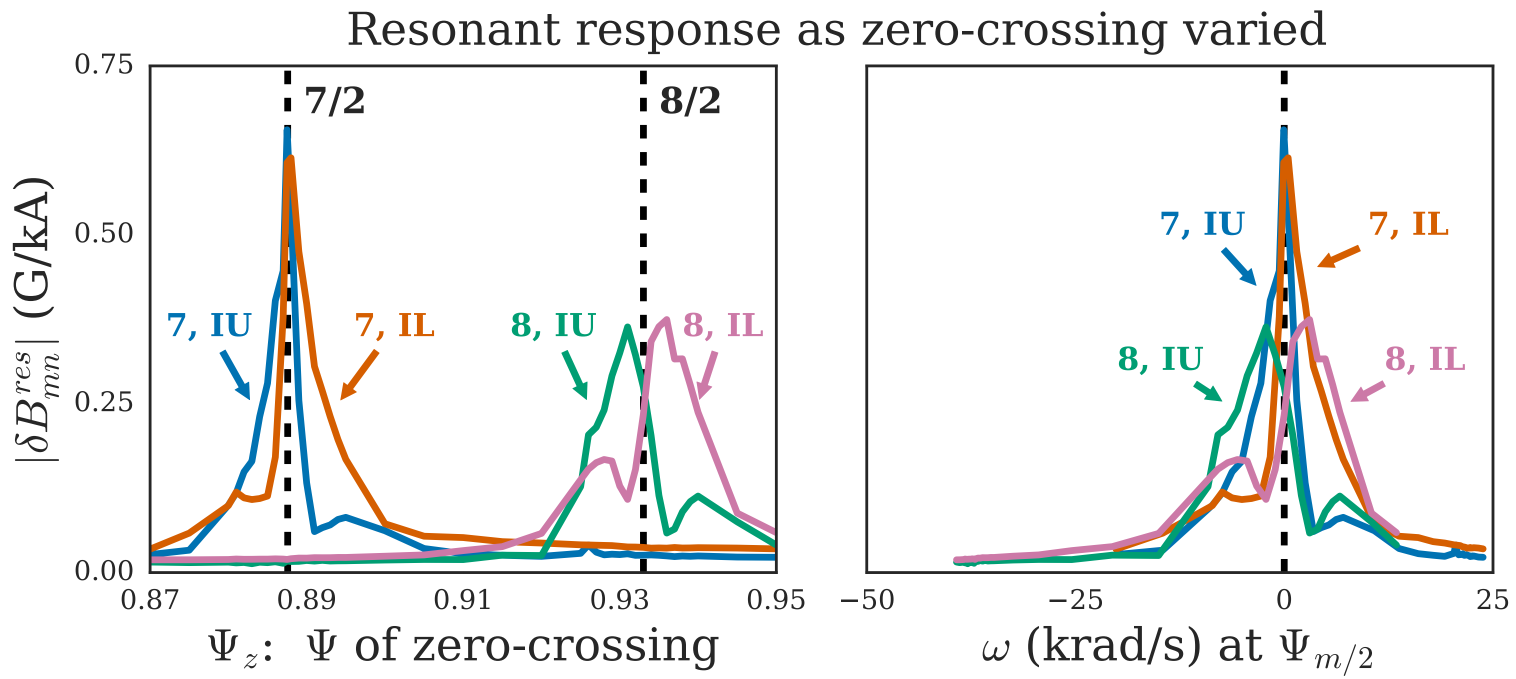

- **Resonant field amplified when zero-crossing aligns with rational surface**
- Resonant field peaks for | ω | < 10 krad/s at rational surface
- Response almost always screened below vacuum level
- Resonant response exhibits fine structure
  - IU and IL response weighted to opposite sides of surface
  - Multiple peaks clearly visible at q=8/2

Low rotation increases resonant response

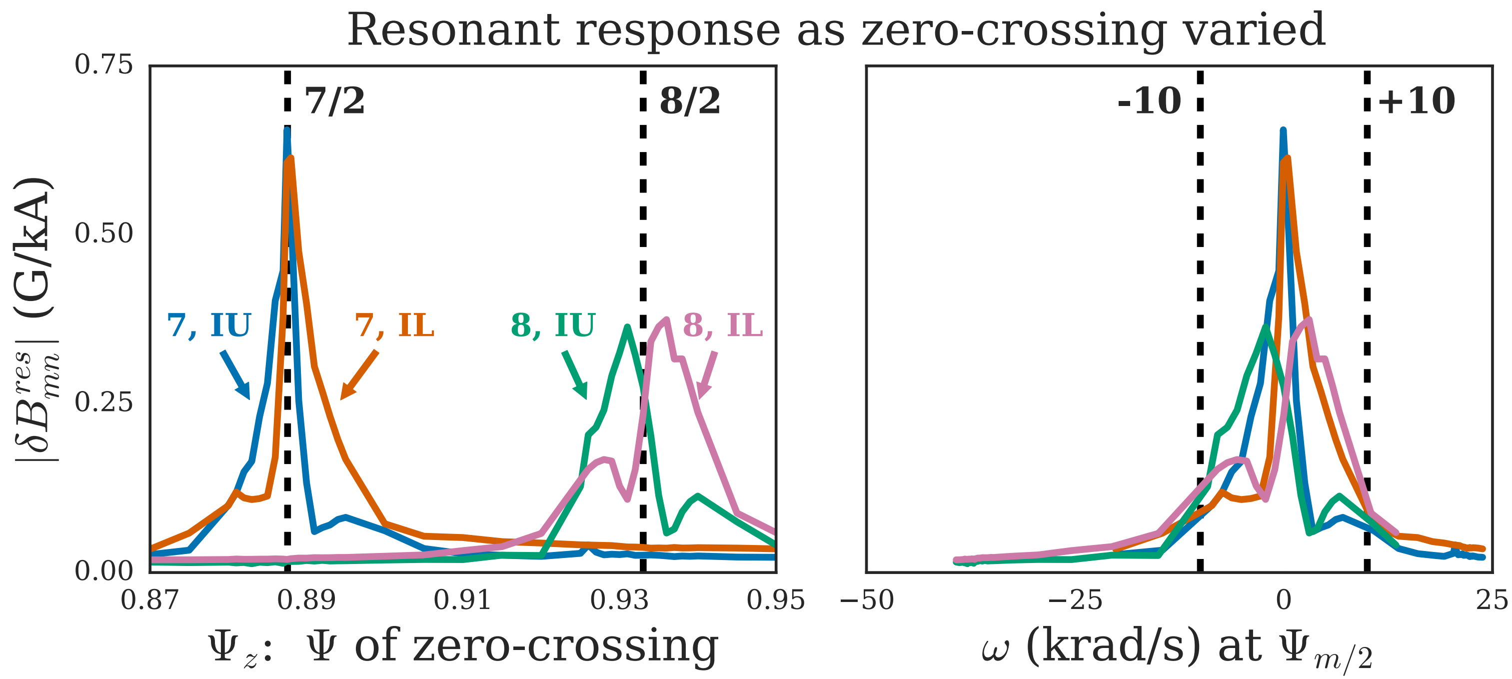

- **Resonant field amplified when zero-crossing aligns with rational surface**
- **Resonant field peaks for | ω | < 10 krad/s at rational surface**
- Response almost always screened below vacuum level
- Resonant response exhibits fine structure
  - IU and IL response weighted to opposite sides of surface
  - Multiple peaks clearly visible at q=8/2

Low rotation increases resonant response

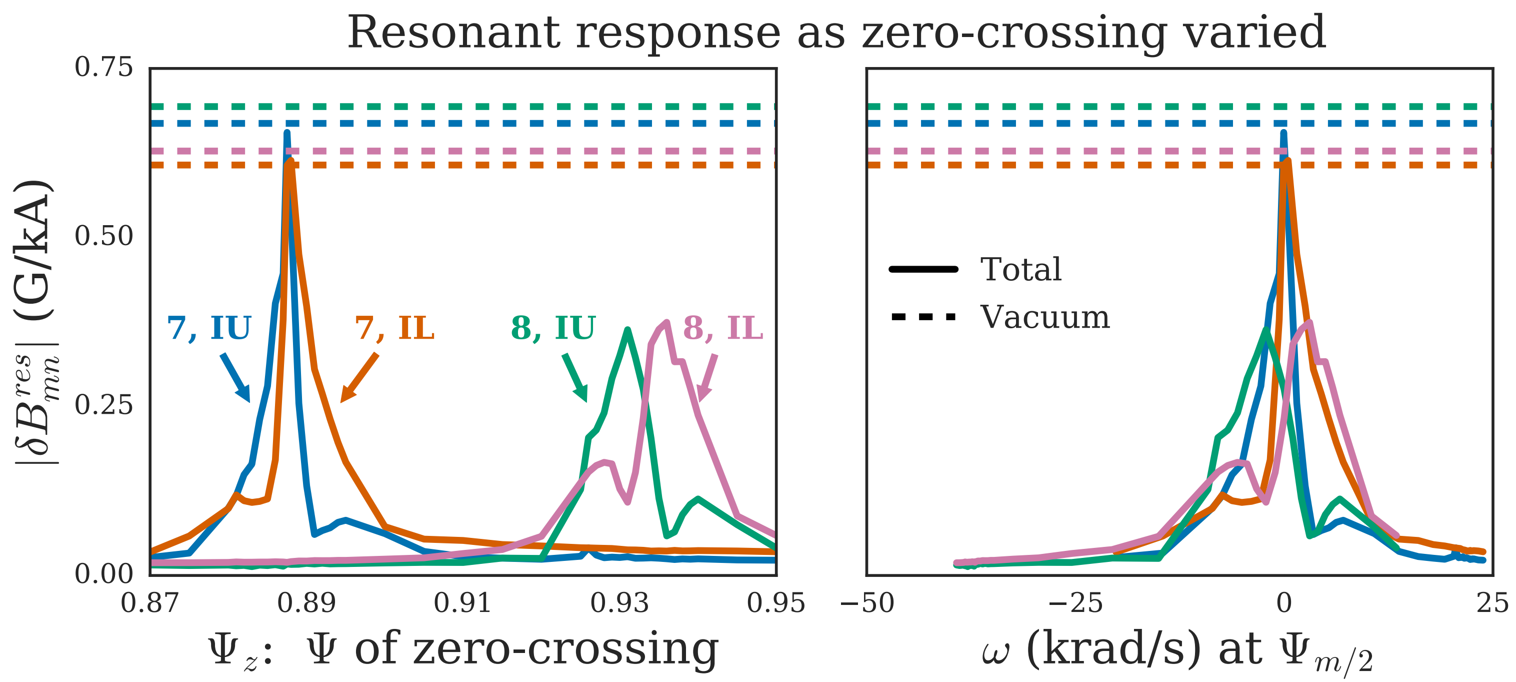

- **Resonant field amplified when zero-crossing aligns with rational surface**
- **Resonant field peaks for | ω | < 10 krad/s at rational surface**
- **Response almost always screened below vacuum level**
- **Resonant response exhibits fine structure**
  - IU and IL response weighted to opposite sides of surface
  - Multiple peaks clearly visible at q=8/2

OAK RIDGE INSTITUTE FOR SCIENCE AND EDUCATION
Managed by ORAU for DOE

GENERAL ATOMICS

Low rotation increases resonant response

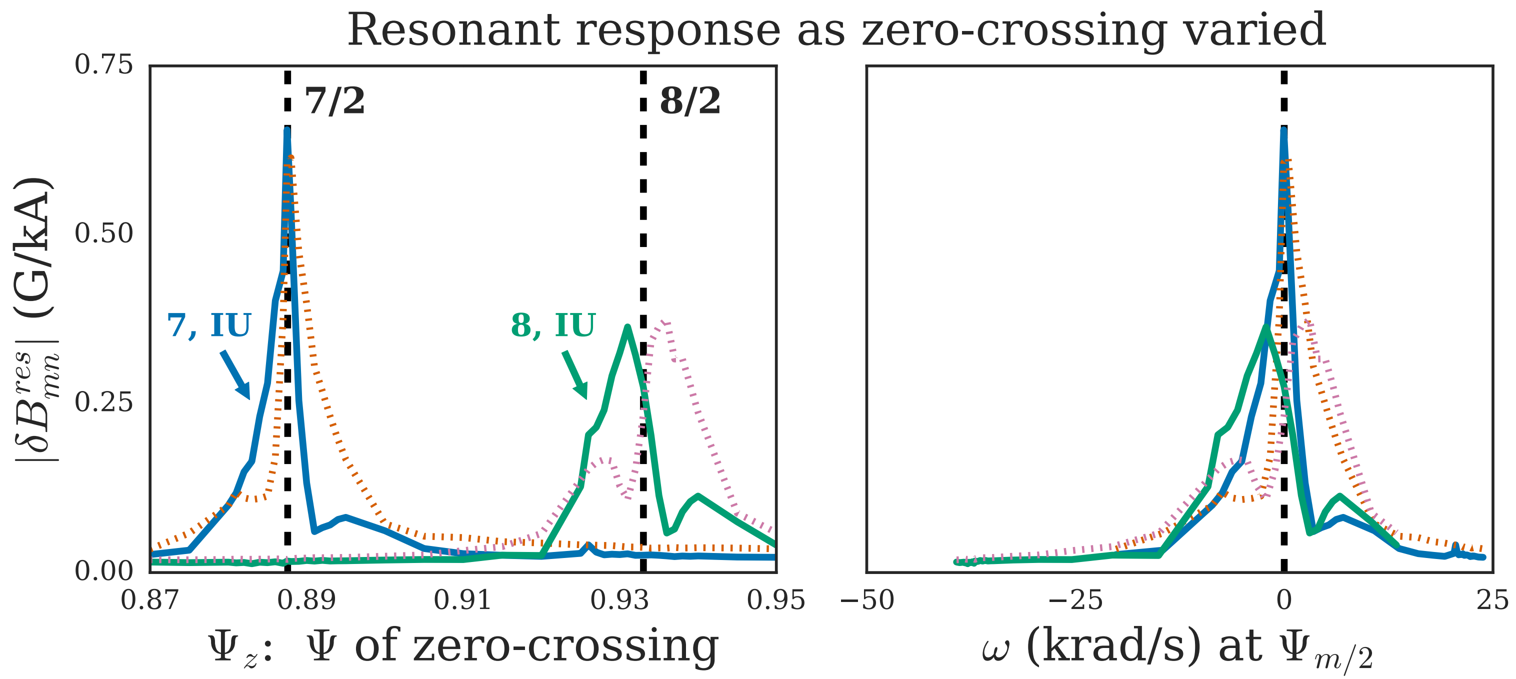

- **Resonant field amplified when zero-crossing aligns with rational surface**
- **Resonant field peaks for | ω | < 10 krad/s at rational surface**
- **Response almost always screened below vacuum level**
- **Resonant response exhibits fine structure**
  - IU and IL response weighted to opposite sides of surface
  - Multiple peaks clearly visible at q=8/2

Low rotation increases resonant response

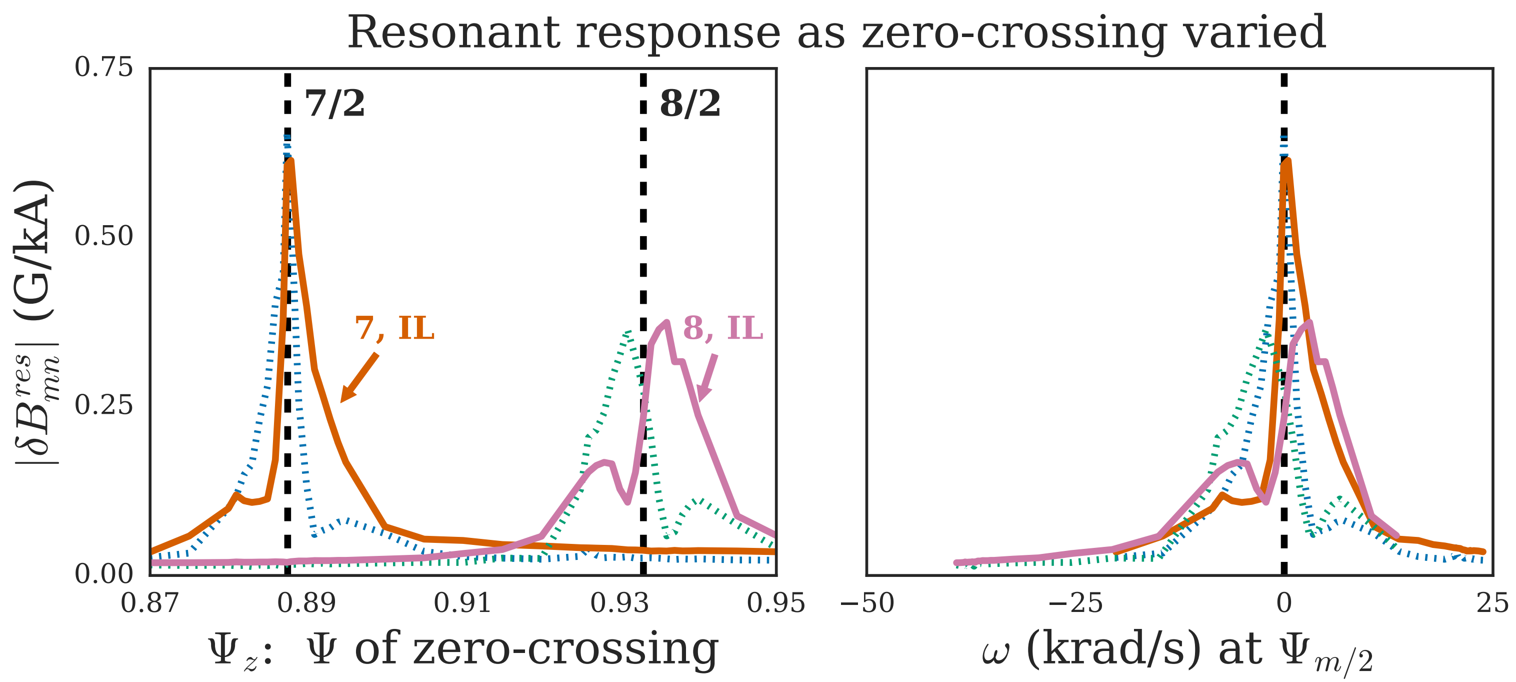

- **Resonant field amplified when zero-crossing aligns with rational surface**
- **Resonant field peaks for | ω | < 10 krad/s at rational surface**
- **Response almost always screened below vacuum level**
- **Resonant response exhibits fine structure**
  - IU and IL response weighted to opposite sides of surface
  - Multiple peaks clearly visible at q=8/2

Low rotation increases resonant response

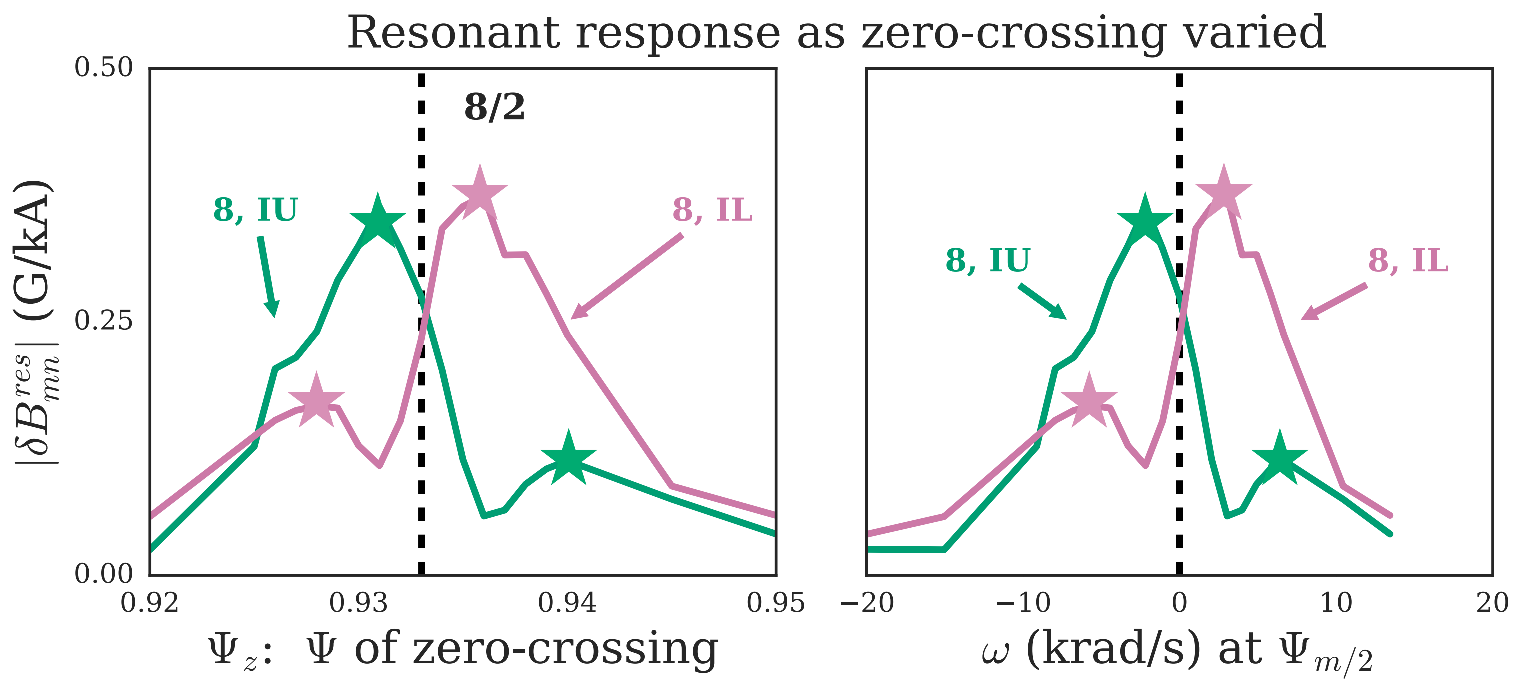

- **Resonant field amplified when zero-crossing aligns with rational surface**
- **Resonant field peaks for $|\omega|$ < 10 krad/s at rational surface**
- **Response almost always screened below vacuum level**
- **Resonant response exhibits fine structure**
  - IU and IL response weighted to opposite sides of surface
  - Multiple peaks clearly visible at q=8/2

Zero-crossing induces broad coupling of Fourier components of perturbed magnetic field

- **Coupling occurs regardless of whether zero-crossing is on resonant surface or in between**
- Near-resonant Fourier components are amplified
- Far-off-resonant Fourier components decrease
- Appears as streak across *m* in SURFMN-like diagrams

Ψ_z=0.888
q=7/2

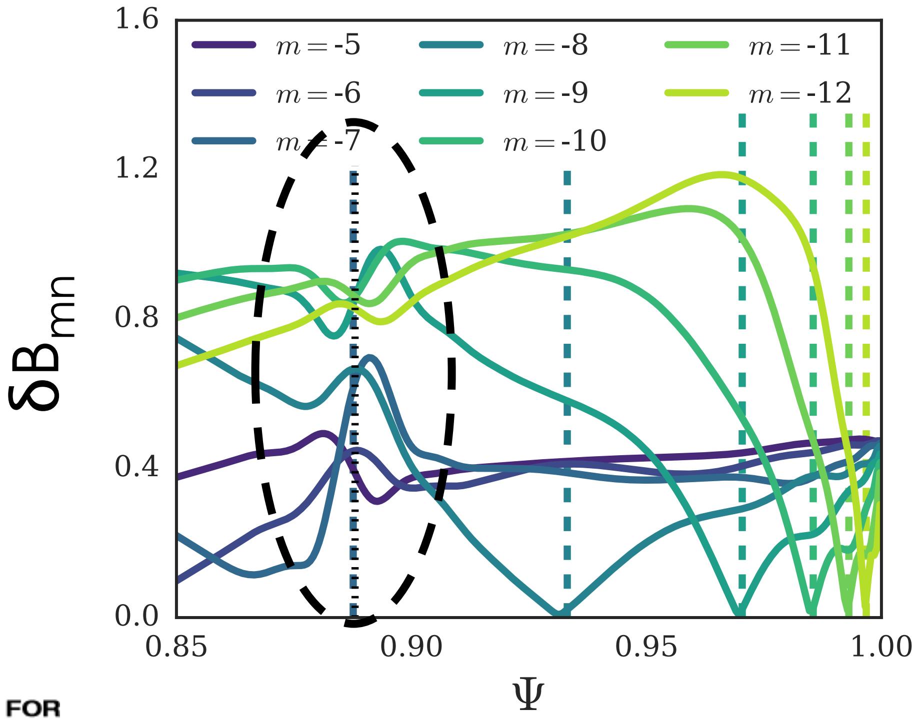

OAK RIDGE INSTITUTE FOR SCIENCE AND EDUCATION
Managed by ORAU for DOE

GENERAL ATOMICS

Zero-crossing induces broad coupling of Fourier components of perturbed magnetic field

- **Coupling occurs regardless of whether zero-crossing is on resonant surface or in between**
- Near-resonant Fourier components are amplified
- Far-off-resonant Fourier components decrease
- Appears as streak across *m* in SURFMN-like diagrams

Ψ_z=0.915

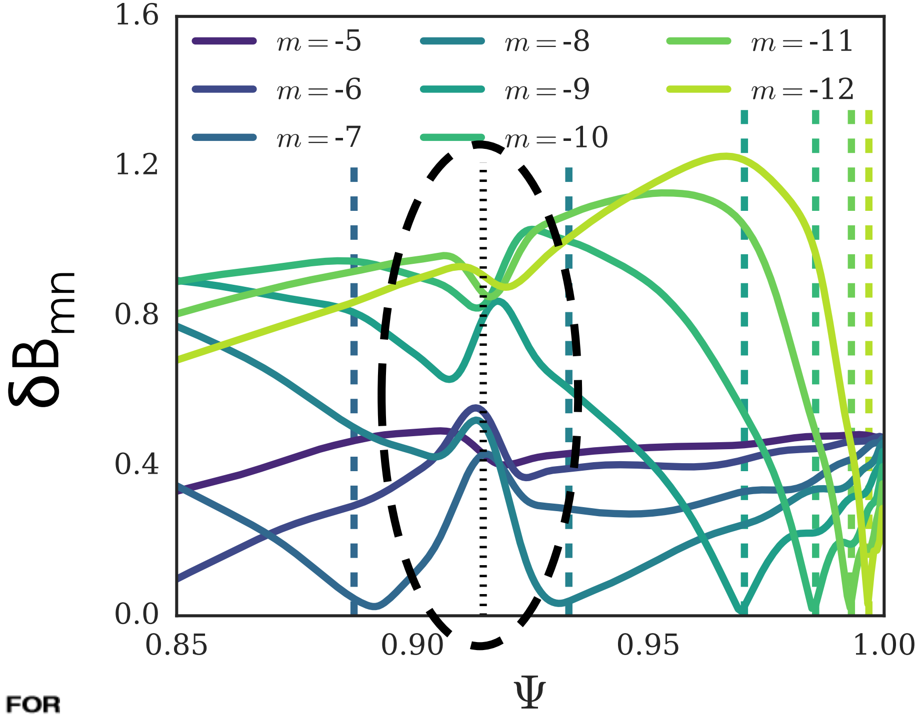

OAK RIDGE INSTITUTE FOR SCIENCE AND EDUCATION
Managed by ORAU for DOE

GENERAL ATOMICS

Zero-crossing induces broad coupling of Fourier components of perturbed magnetic field

- **Coupling occurs regardless of whether zero-crossing is on resonant surface or in between**
- Near-resonant Fourier components are amplified
- Far-off-resonant Fourier components decrease
- Appears as streak across *m* in SURFMN-like diagrams

Ψ_z=0.933
q=8/2

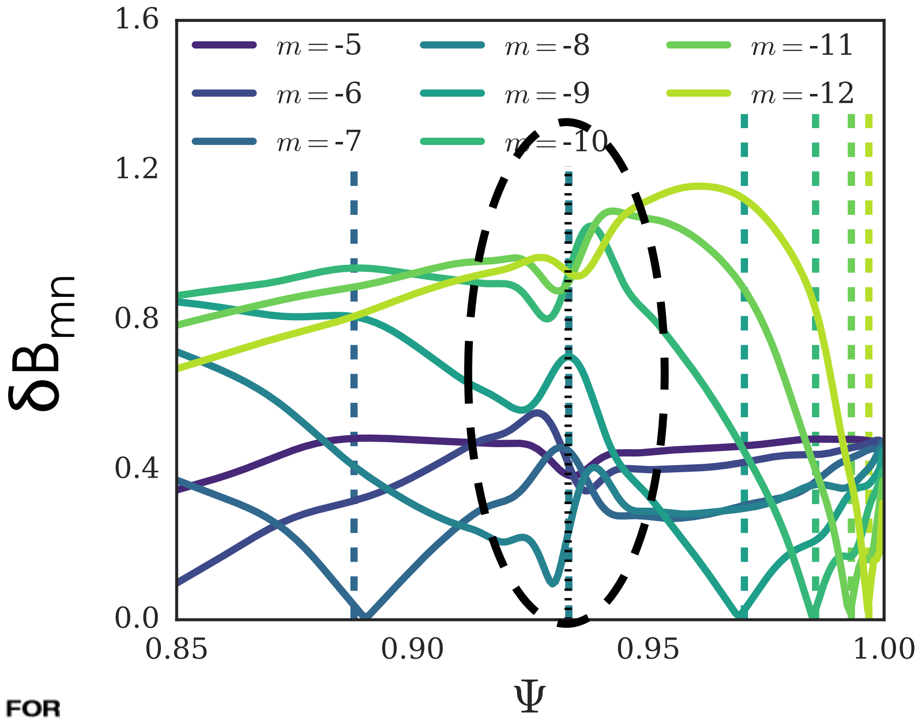

OAK RIDGE INSTITUTE FOR SCIENCE AND EDUCATION
Managed by ORAU for DOE

GENERAL ATOMICS

Zero-crossing induces broad coupling of Fourier components of perturbed magnetic field

- **Coupling occurs regardless of whether zero-crossing is on resonant surface or in between**
- **Near-resonant Fourier components are amplified**
- Far-off-resonant Fourier components decrease
- Appears as streak across *m* in SURFMN-like diagrams

Ψ_z=0.915

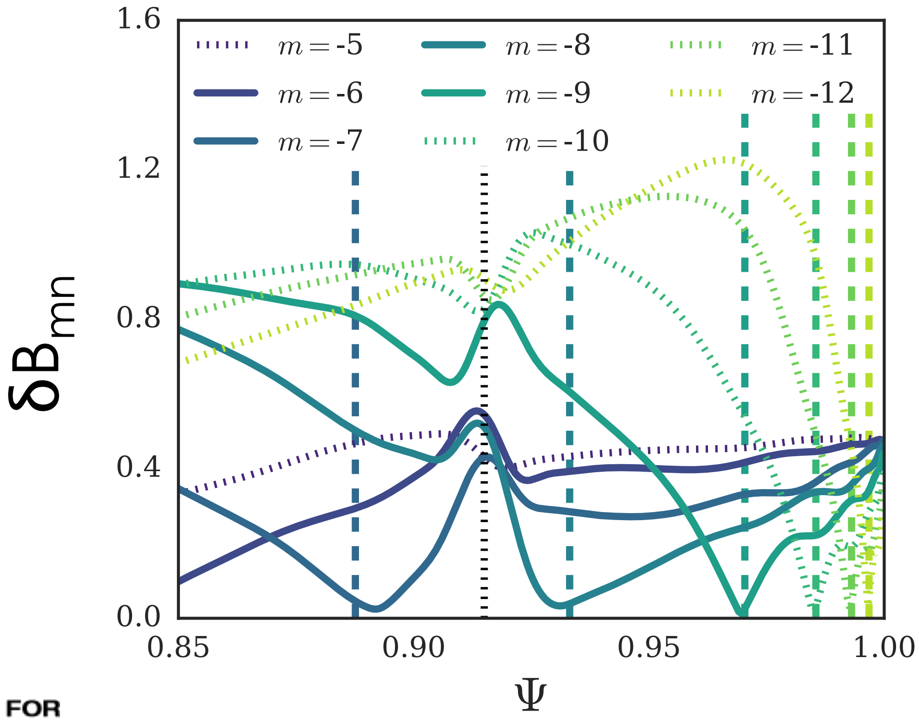

OAK RIDGE INSTITUTE FOR SCIENCE AND EDUCATION
Managed by ORAU for DOE

GENERAL ATOMICS

Zero-crossing induces broad coupling of Fourier components of perturbed magnetic field

- **Coupling occurs regardless of whether zero-crossing is on resonant surface or in between**
- **Near-resonant Fourier components are amplified**
- **Far-off-resonant Fourier components decrease**
- **Appears as streak across *m* in SURFMN-like diagrams**

Ψ_z=0.915

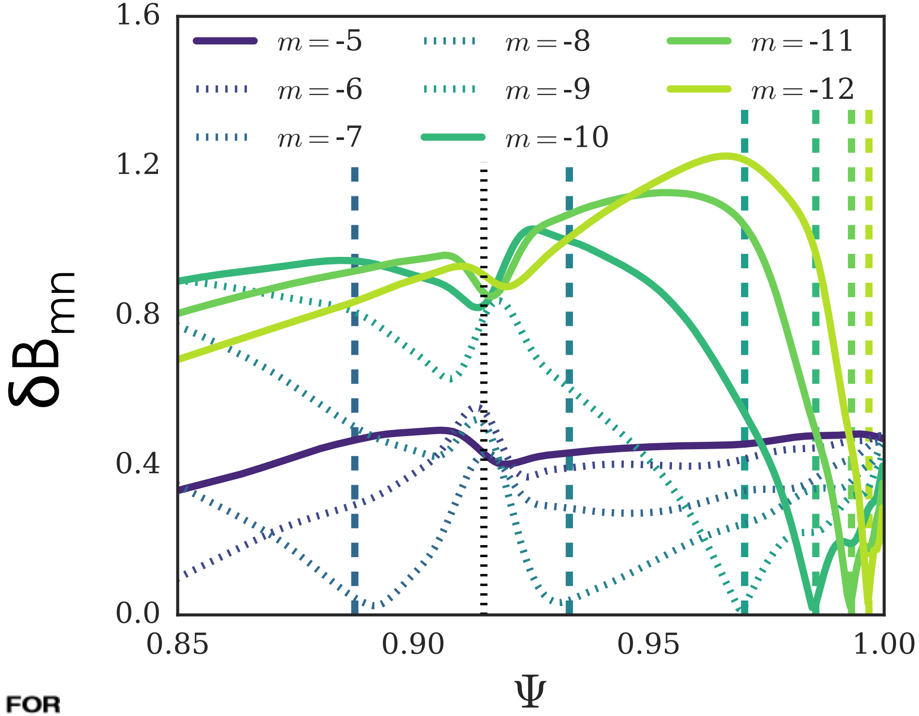

OAK RIDGE INSTITUTE FOR SCIENCE AND EDUCATION
Managed by ORAU for DOE

GENERAL ATOMICS

Zero-crossing induces broad coupling of Fourier components of perturbed magnetic field

- **Coupling occurs regardless of whether zero-crossing is on resonant surface or in between**
- **Near-resonant Fourier components are amplified**
- **Far-off-resonant Fourier components decrease**
- **Appears as streak across *m* in SURFMN-like diagrams**

Ψ_z=0.915

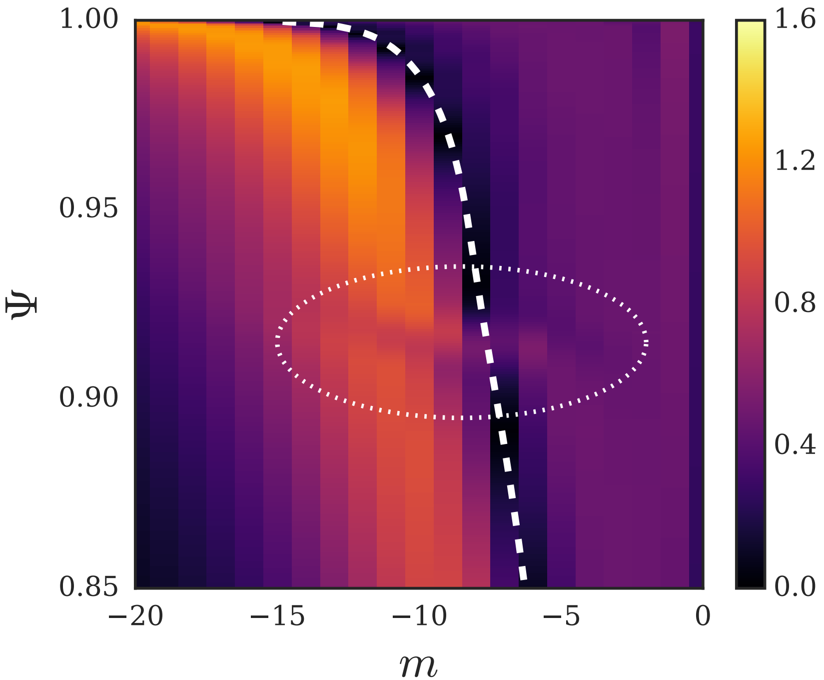

OAK RIDGE INSTITUTE FOR SCIENCE AND EDUCATION
Managed by ORAU for DOE

GENERAL ATOMICS

Coupling caused by current induced by mode driven at zero-crossing

Fourier decomposition of parallel current shows near-resonant nature of mode

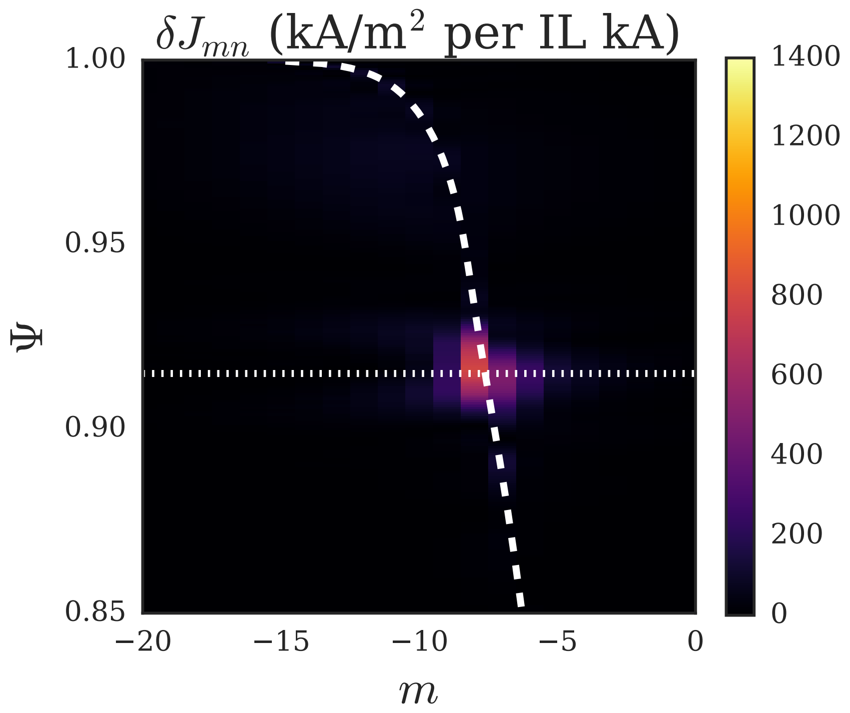

Significant rotation shear required to drive mode

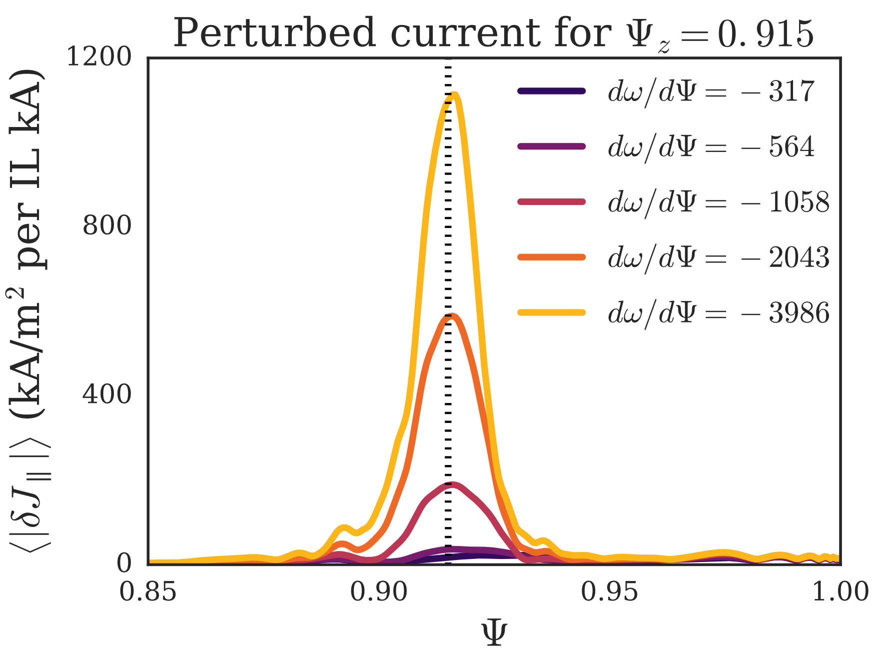

OAK RIDGE INSTITUTE FOR SCIENCE AND EDUCATION
Managed by ORAU for DOE

GENERAL ATOMICS

Observability of plasma response

Changes to plasma response observable by high-field side magnetic probes

- **Magnetic sensors can measure poloidal field at low-field side (LFS) and high-field side (HFS) midplane**
- HFS signals show
  - Up to 50% magnitude change
  - 20° - 45° phase shift
    - Localized around q=7/2
    - "Permanent" across q=8/2
- LFS signals show much smaller degree of variation

δB_Z: Even-parity plasma response

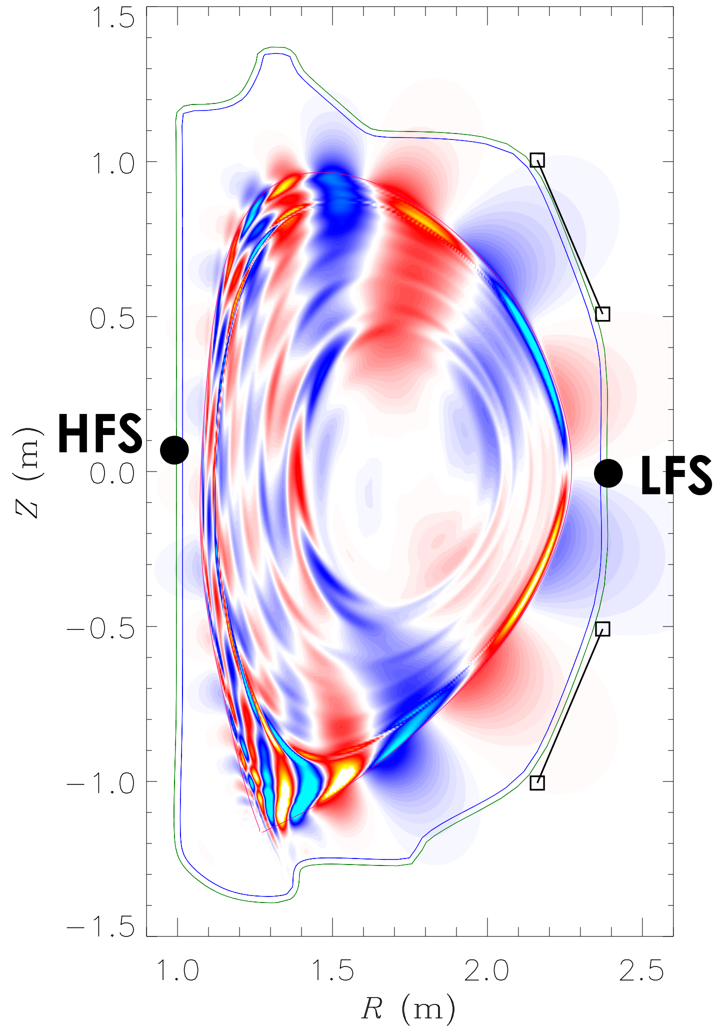

OAK RIDGE INSTITUTE FOR SCIENCE AND EDUCATION
Managed by ORAU for DOE

GENERAL ATOMICS

Changes to plasma response observable by high-field side magnetic probes

- **Magnetic sensors can measure poloidal field at low-field side (LFS) and high-field side (HFS) midplane**
- **HFS signals show**
  - Up to 50% magnitude change
  - 20° - 45° phase shift
    - Localized around q=7/2
    - "Permanent" across q=8/2
- **LFS signals show much smaller degree of variation**

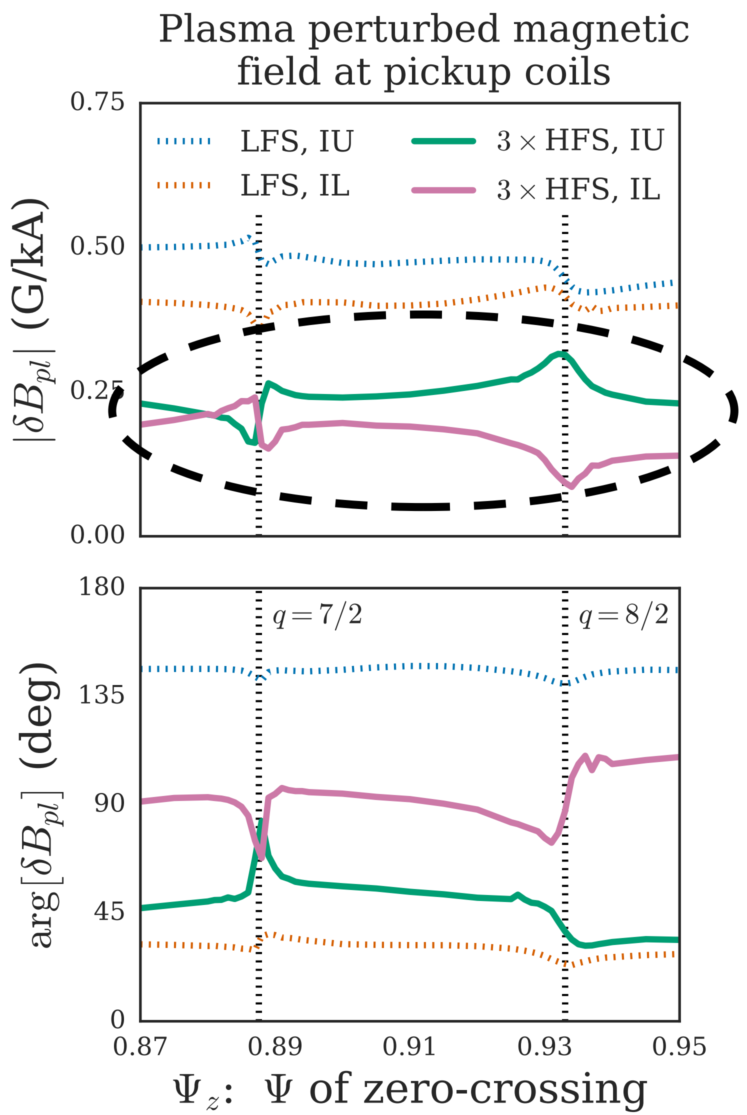

OAK RIDGE INSTITUTE FOR SCIENCE AND EDUCATION
Managed by ORAU for DOE

GENERAL ATOMICS

Changes to plasma response observable by high-field side magnetic probes

- **Magnetic sensors can measure poloidal field at low-field side (LFS) and high-field side (HFS) midplane**
- **HFS signals show**
  - Up to 50% magnitude change
  - 20° - 45° phase shift
    - Localized around q=7/2
    - "Permanent" across q=8/2
- **LFS signals show much smaller degree of variation**

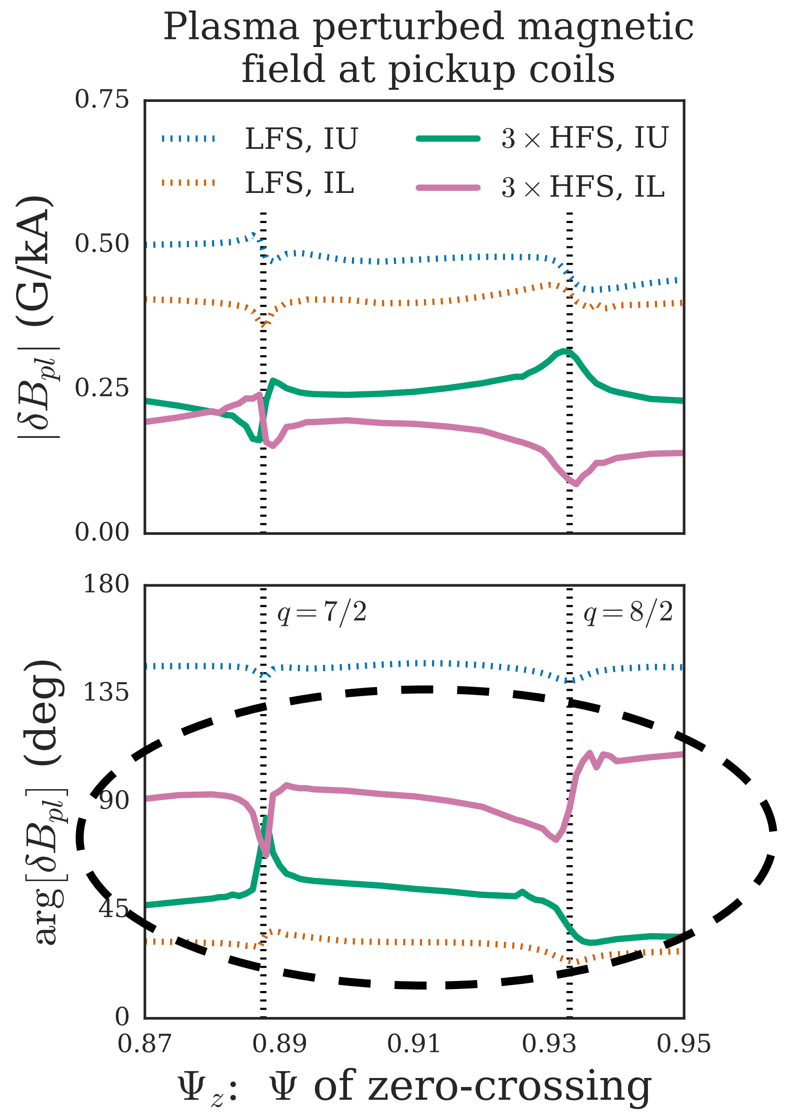

OAK RIDGE INSTITUTE FOR SCIENCE AND EDUCATION
Managed by ORAU for DOE

GENERAL ATOMICS

Changes to plasma response observable by high-field side magnetic probes

- **Magnetic sensors can measure poloidal field at low-field side (LFS) and high-field side (HFS) midplane**
- **HFS signals show**
  - Up to 50% magnitude change
  - 20° - 45° phase shift
    - Localized around q=7/2
    - "Permanent" across q=8/2
- **LFS signals show much smaller degree of variation**

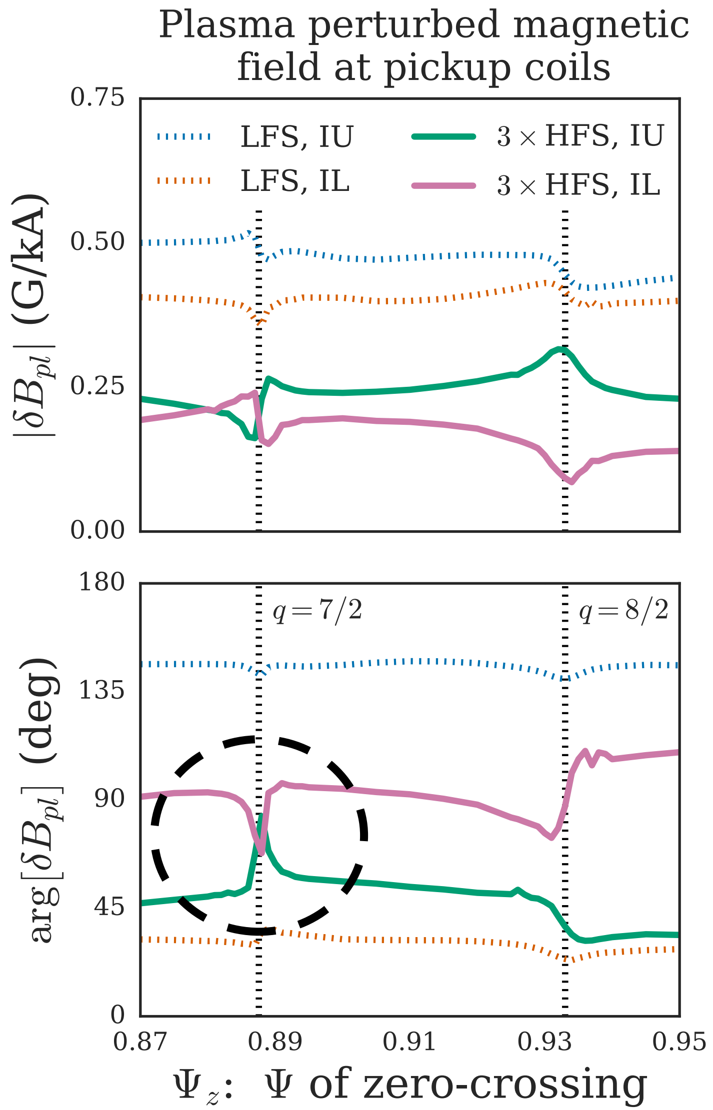

Changes to plasma response observable by high-field side magnetic probes

- **Magnetic sensors can measure poloidal field at low-field side (LFS) and high-field side (HFS) midplane**
- **HFS signals show**
  - Up to 50% magnitude change
  - 20° - 45° phase shift
    - Localized around q=7/2
    - "Permanent" across q=8/2
- LFS signals show much smaller degree of variation

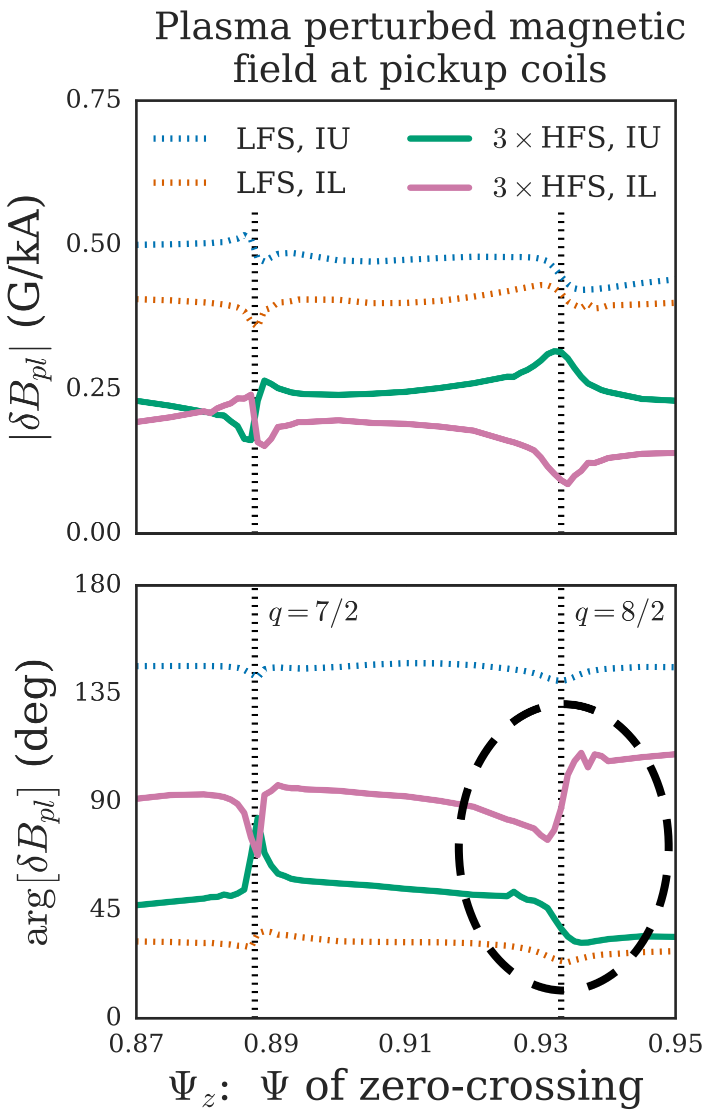

Changes to plasma response observable by high-field side magnetic probes

- **Magnetic sensors can measure poloidal field at low-field side (LFS) and high-field side (HFS) midplane**
- **HFS signals show**
  - Up to 50% magnitude change
  - 20° - 45° phase shift
    - Localized around q=7/2
    - "Permanent" across q=8/2
- **LFS signals show much smaller degree of variation**

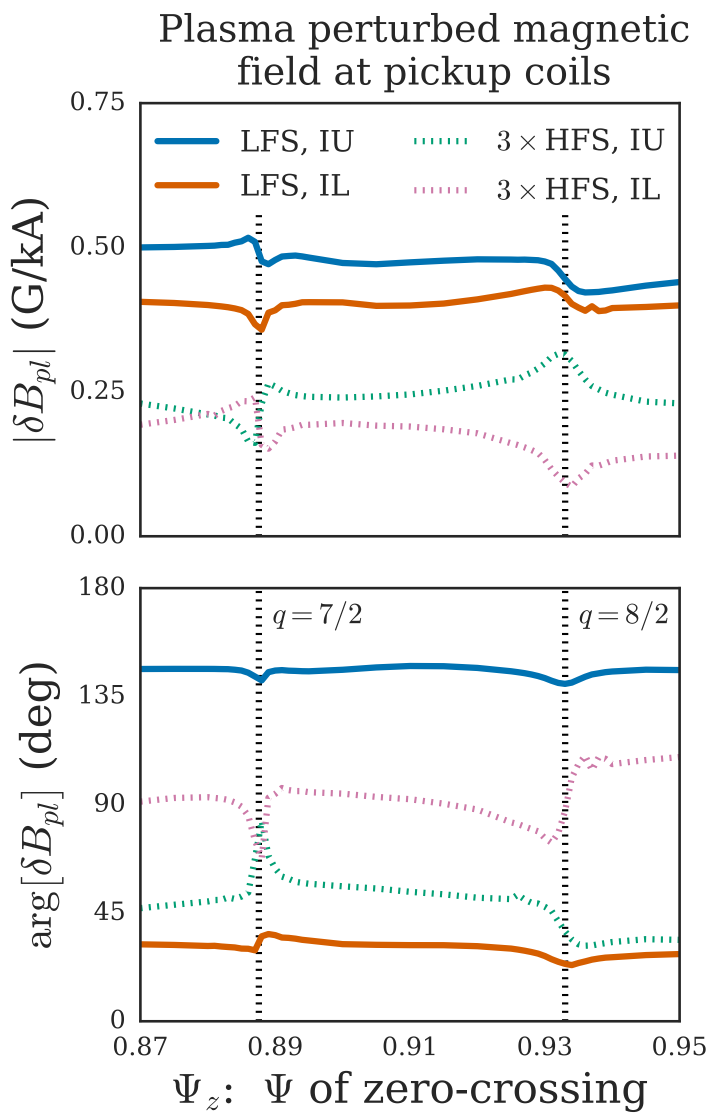

Divertor footprints are insensitive to these changes

- **Divertor footprint structure calculated with coupled:**
  - TRIP3D (field line integration)
  - MAFOT (invariant manifold)
- **Simulations show little change as zero-crossing is varied**
- **Strike point splitting observed in experiments may be modified by plasma response closer to edge**

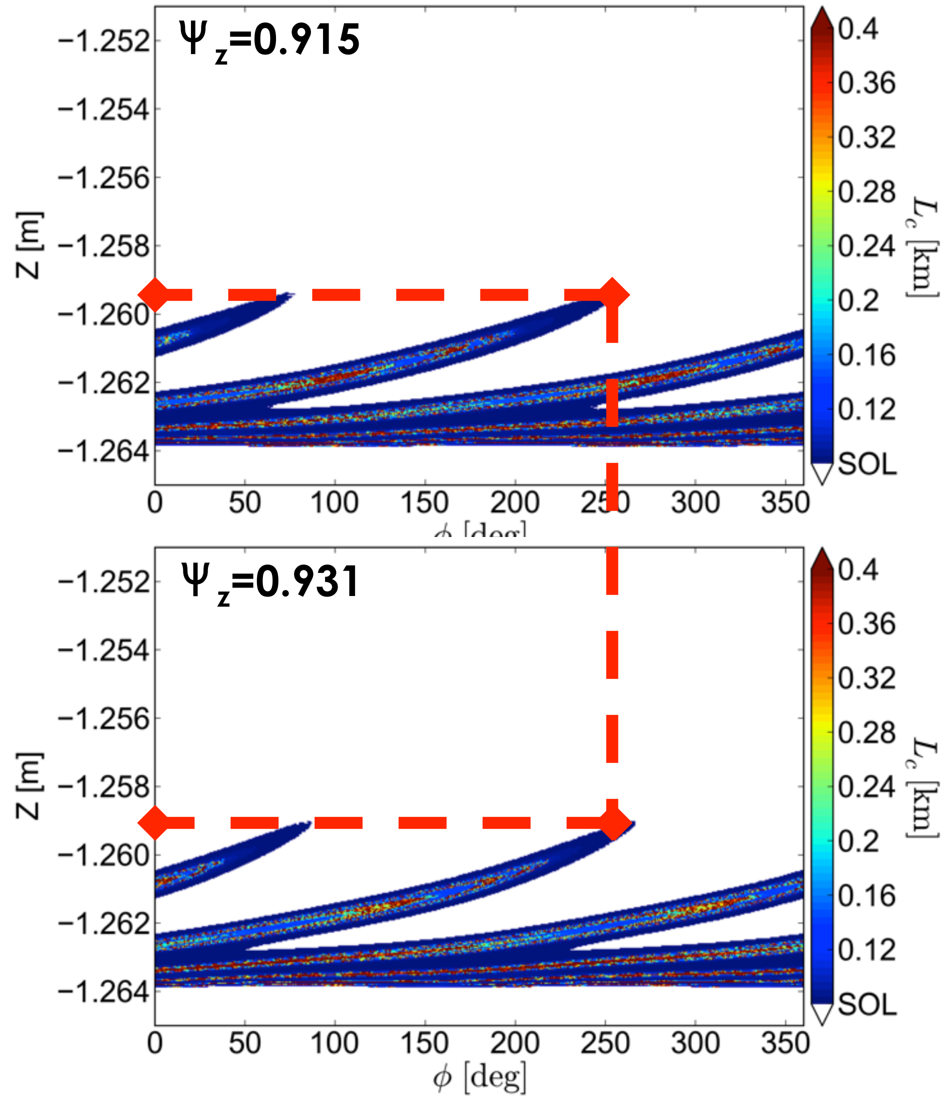

OAK RIDGE INSTITUTE FOR SCIENCE AND EDUCATION
Managed by ORAU for DOE

GENERAL ATOMICS

Quasilinear electromagnetic torque

Quasilinear torque density from non-resonant response acts to flatten rotation profile

- **Negative torque inside zero-crossing decreases positive rotation**
- **Positive torque outside zero-crossing increases negative rotation**
- **ELM-suppression hypothesis**
  - Reduced shear destabilizes turbulent modes
  - Increased transport arrests growth of pedestal height and width

$$\tau\left(\Psi\right) = \left\langle R^2 \nabla\varphi \cdot \left(\delta\mathbf{J} \times \delta\mathbf{B}\right)\right\rangle$$

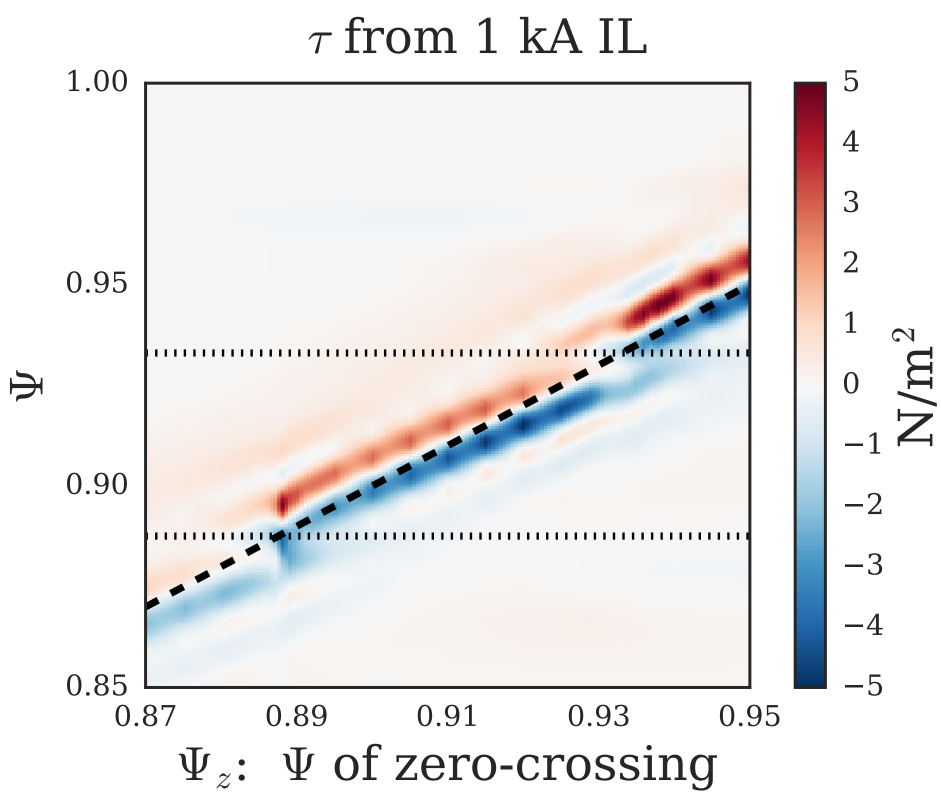

Quasilinear torque density from non-resonant response drives zero-crossing toward rational surfaces

- **Negative torque at Ψ_z**
  - Drives negative rotation
  - Zero-crossing moves inward
- **Positive torque at Ψ_z**
  - Drives positive rotation
  - Zero-crossing moves outward
- **"Stable points" exist in vicinity of rational surface**
- **ELM-suppression hypothesis**
  - Torque locks zero-crossing close to rational surface
  - Low rotation permits increased resonant field
  - Island penetration leads to ELM-suppression bifurcation

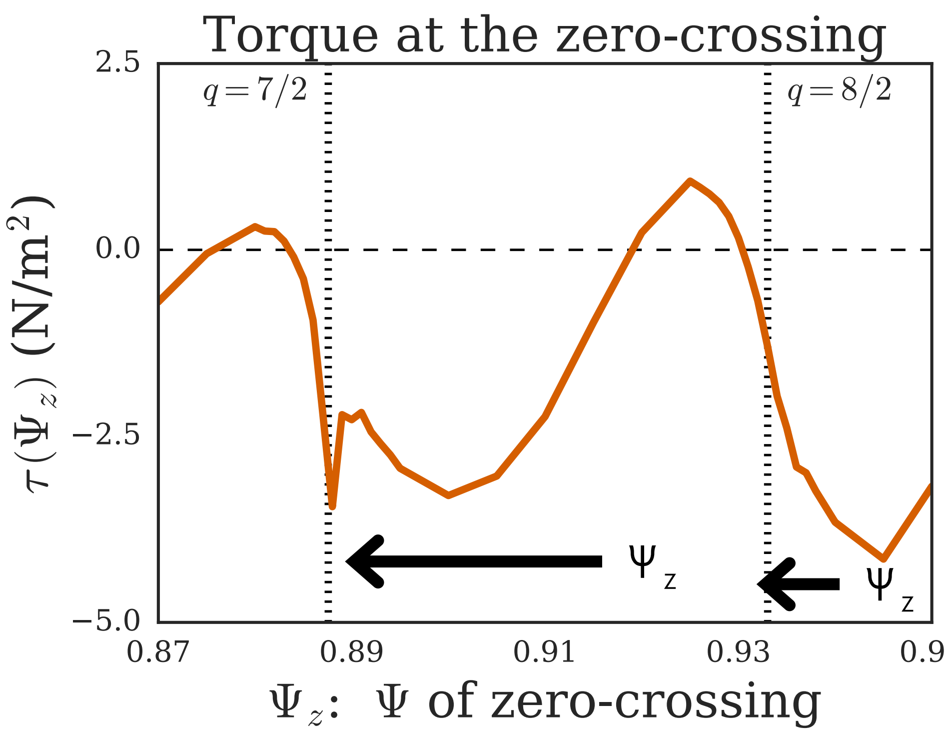

Torque from IL response

Quasilinear torque density from non-resonant response drives zero-crossing toward rational surfaces

- **Negative torque at Ψ_z**
  - Drives negative rotation
  - Zero-crossing moves inward
- **Positive torque at Ψ_z**
  - Drives positive rotation
  - Zero-crossing moves outward
- **"Stable points" exist in vicinity of rational surface**
- **ELM-suppression hypothesis**
  - Torque locks zero-crossing close to rational surface
  - Low rotation permits increased resonant field
  - Island penetration leads to ELM-suppression bifurcation

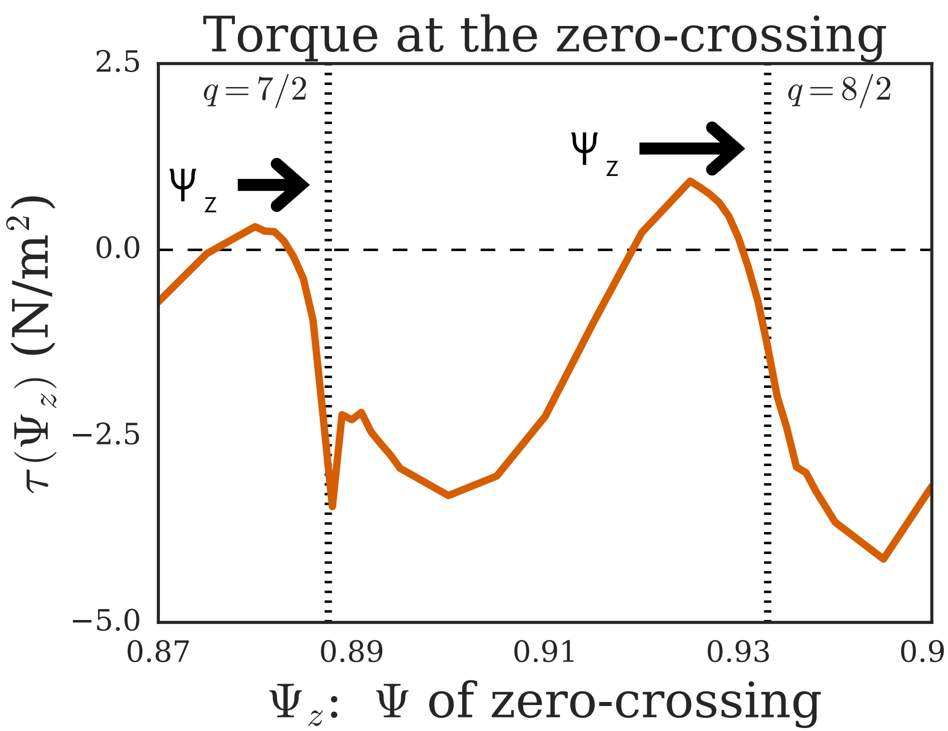

Torque from IL response

Quasilinear torque density from non-resonant response drives zero-crossing toward rational surfaces

- **Negative torque at Ψ_z**
  - Drives negative rotation
  - Zero-crossing moves inward
- **Positive torque at Ψ_z**
  - Drives positive rotation
  - Zero-crossing moves outward
- **"Stable points" exist in vicinity of rational surface**
- **ELM-suppression hypothesis**
  - Torque locks zero-crossing close to rational surface
  - Low rotation permits increased resonant field
  - Island penetration leads to ELM-suppression bifurcation

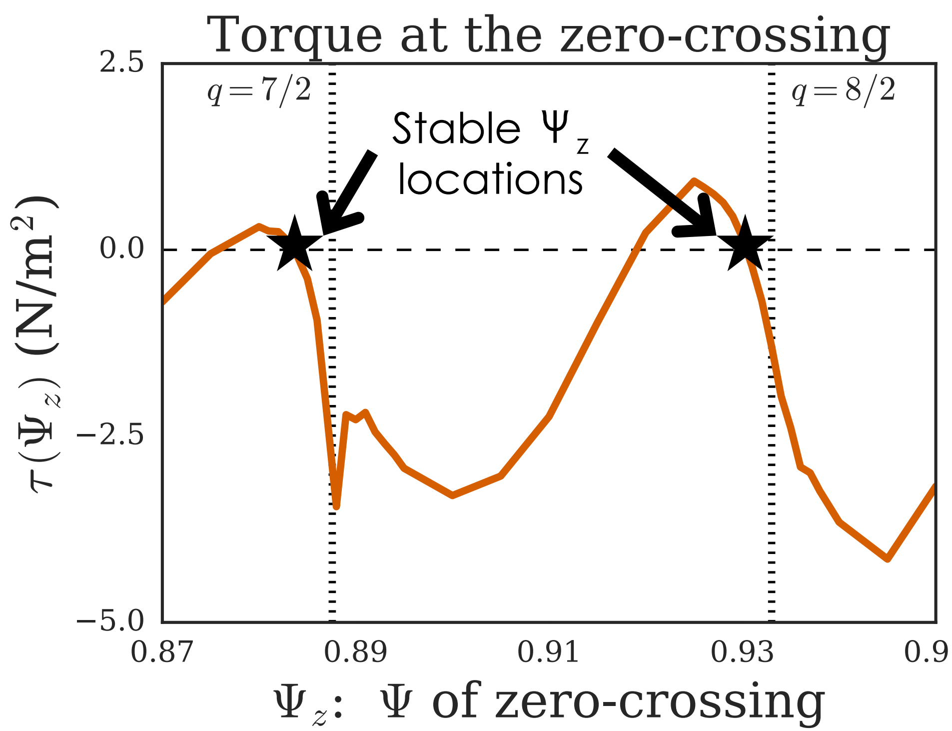

Torque from IL response

OAK RIDGE INSTITUTE FOR SCIENCE AND EDUCATION
Managed by ORAU for DOE

GENERAL ATOMICS

Quasilinear torque density from non-resonant response drives zero-crossing toward rational surfaces

- **Negative torque at Ψ_z**
  - Drives negative rotation
  - Zero-crossing moves inward
- **Positive torque at Ψ_z**
  - Drives positive rotation
  - Zero-crossing moves outward
- **"Stable points" exist in vicinity of rational surface**
- **ELM-suppression hypothesis**
  - Torque locks zero-crossing close to rational surface
  - Low rotation permits increased resonant field
  - Island penetration leads to ELM-suppression bifurcation

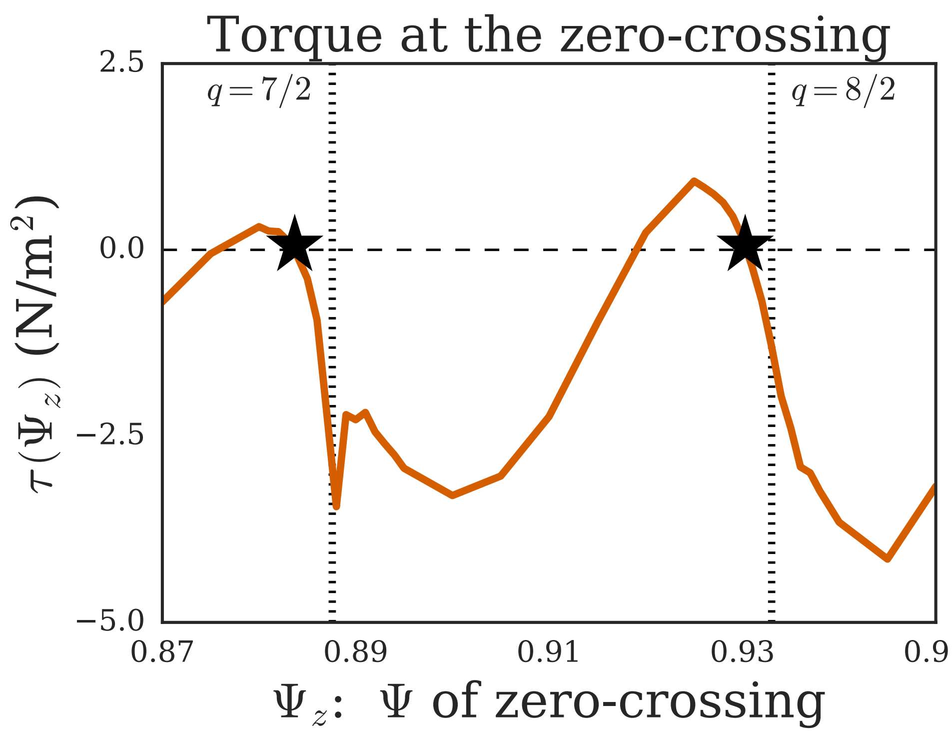

Torque from IL response

Summary

- **Resonant and non-resonant plasma response sensitive to rotation zero-crossing**
- **Changes to resonant response should be observable by HFS magnetic sensors**
- **Quasilinear torque from near-resonant mode may play an important role in ELM-suppression**
  - Reduced shear causes increased turbulent transport
  - Zero-crossing driven toward rational surface permits island penetration
- **Future work**
  - Further investigation of hypothesized ELM-suppression mechanisms
  - Scan of edge rotation profile
  - Detailed study of two-fluid effects, including rotation scan

Acknowledgments

- This research was supported by the U.S. Department of Energy Fusion Energy Sciences Postdoctoral Research Program administered by the Oak Ridge Institute for Science and Education (ORISE) for the DOE. ORISE is managed by Oak Ridge Associated Universities (ORAU) under DOE contract number DE-AC05-06OR23100. All opinions expressed in this presentation are the authors' and do not necessarily reflect the policies and views of DOE, ORAU, or ORISE.
- This work was sponsored by the U.S. Department of Energy under grant nos. DE-FG02-95ER54309 and DE-FC02-06ER54873 and the SciDAC Center for Extended Magnetohydrodynamic Modeling (CEMM).